

Combination of Triple Bond and Adamantane Ring on the Vitamin D Side Chain Produced Partial Agonists for Vitamin D Receptor

Takeru Kudo,[†] Michiyasu Ishizawa,^{§,⊥} Kazuki Maekawa,^{†,⊥} Makoto Nakabayashi,^{||,§} Yusuke Watarai,[†] Hikaru Uchida,[§] Hiroaki Tokiwa,^{‡,†} Teikichi Ikura,[#] Nobutoshi Ito,[#] Makoto Makishima,^{*,§} and Sachiko Yamada^{*,§}

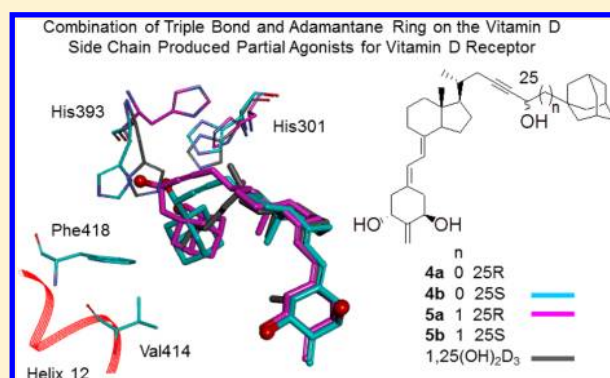
[†]Department of Chemistry, [‡]Research Center for Smart Molecules, Faculty of Science, Rikkyo University, Toshima-ku, Tokyo 171-8501, Japan

[§]Department of Biomedical Sciences, Nihon University School of Medicine, Itabashi-ku, Tokyo 173-8610, Japan

^{||}Graduate School of Biomedical Science and [#]Medical Research Institute, Tokyo Medical and Dental University, Bunkyo-ku, Tokyo 113-8510, Japan

Supporting Information

ABSTRACT: Vitamin D receptor (VDR) ligands are therapeutic agents that are used for the treatment of psoriasis, osteoporosis, and secondary hyperparathyroidism and have immense potential as therapeutic agents for autoimmune diseases, cancers, and cardiovascular diseases. However, the major side effect of VDR ligands, the development of hypercalcemia, limits their expanded use. To develop tissue-selective VDR modulators, we have designed vitamin D analogues with an adamantane ring at the side chain terminal, which would interfere with helix 12, the activation function 2, and modulate the VDR potency. Here we report 25- or 26-adamantyl-23,23,24,24-tetrahydro-19-norvitamin D derivatives (ADTK1–4, **4b**, **a** and **5a**, **b**). These compounds showed high VDR affinities (90% at maximum), partial agonistic activities (EC_{50} 10^{-9} – 10^{-8} M with 40–80% efficacy) in trans-activation, and tissue-selective activity in target gene expressions. We investigate the structure–activity relationships of these compounds on the basis of their X-ray crystal structures.



INTRODUCTION

The fundamental actions of the steroid hormone, $1\alpha,25$ -dihydroxyvitamin D₃ [$1,25(\text{OH})_2\text{D}_3$, **1**], are to maintain calcium and phosphorus homeostasis in vertebrate organisms. This activity is initiated by direct binding of the hormone to the vitamin D receptor (VDR), a member of the nuclear receptor superfamily, in the intestine, kidney, and bone. In the intestine and kidney, transepithelial transport of calcium is known to involve the apical calcium ion channels TRPV5 and TRPV6.¹ In contrast, activity in the skeleton is driven primarily by RANKL, a TNF-like factor produced by stromal cells and osteoblasts, which are both necessary and sufficient for the formation, activation, and survival of bone-resorbing osteoclasts.² Perhaps most importantly, the primary regulator of TRPV5, TRPV6, and RANKL expression is $1,25(\text{OH})_2\text{D}_3$.

Bone degenerative disease such as osteoporosis occurs in a substantial proportion of the elderly population.³ Osteoporosis encompasses a heterogeneous group of disorders that represents a major risk for bone fractures and a substantial burden on the health care system. More than 15 billion dollars are spent annually in the United State on medical care for the treatment of osteoporosis.⁴ Although a number of antiresorptive agents,

including bisphosphonates, estrogen, and selective estrogen receptor modulators (SERMs), prevent further bone loss, they do not build bone once it has been lost. The US Food and Drug Administration (FDA) has approved a recombinant human parathyroid hormone, also known as teriparatide, as an anabolic bone-building agent for the treatment of osteoporosis.⁵ The FDA also recently approved the anti-RANKL antibody (denosumab)⁶ for the treatment of osteoporosis.

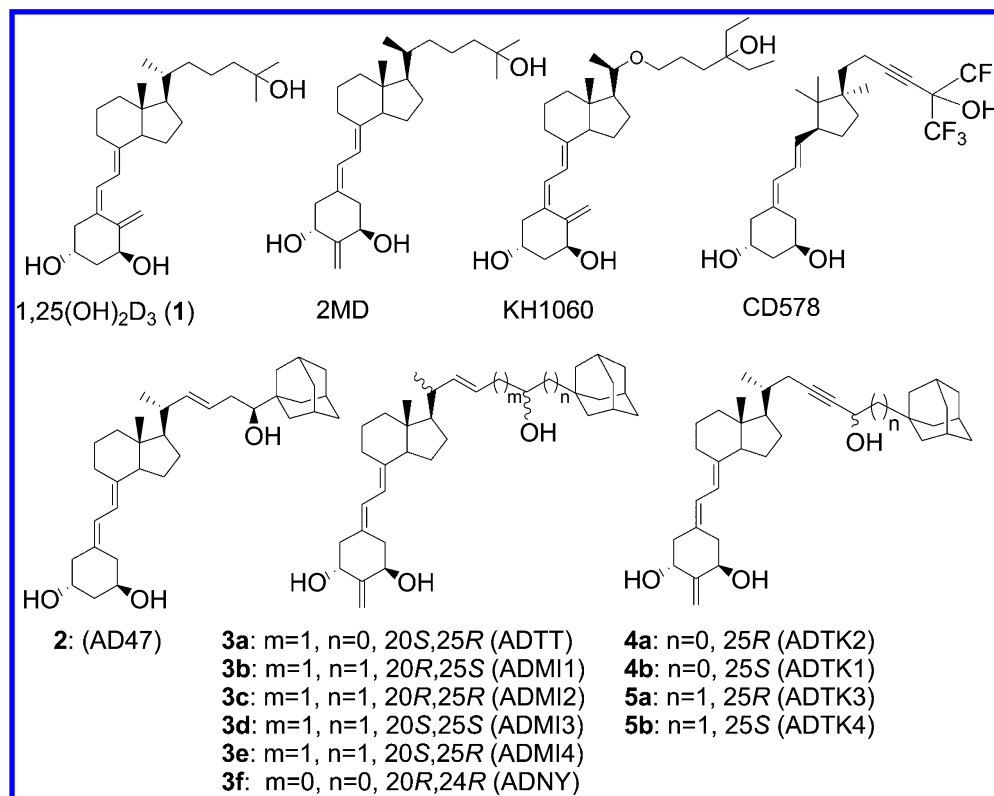
Active vitamin D derivatives have bone anabolic activity⁷ and are naturally derived agents for the treatment of osteoporosis. However, the use of active vitamin D derivatives for the treatment of osteoporosis is difficult because of concerns regarding hypercalcemia and hypercalciuria. Active vitamin D analogues have therefore not yet been approved as osteoporosis agents in the United States and European countries. However, active vitamin D analogues (alfacalcitol and eldcalcitol) have been successfully used in the treatment of osteoporosis in Japan.⁸

Selective VDR modulators can open up possibilities for VDR ligands. 2-Methylene-20-epi-19-norvitamin D (2MD) was first

Received: December 27, 2013

Published: April 28, 2014

Chart 1. Structures of Compounds Discussed in This Article



reported to be a bone-selective anabolic ligand in rats,⁹ however, it was recently shown to increase bone turnover, but not mineral density, in women with osteopenia.¹⁰ Nonsteroidal, non-calcemic, and tissue selective ligands have been reported but still not been proved to be potential therapeutic agents.¹¹

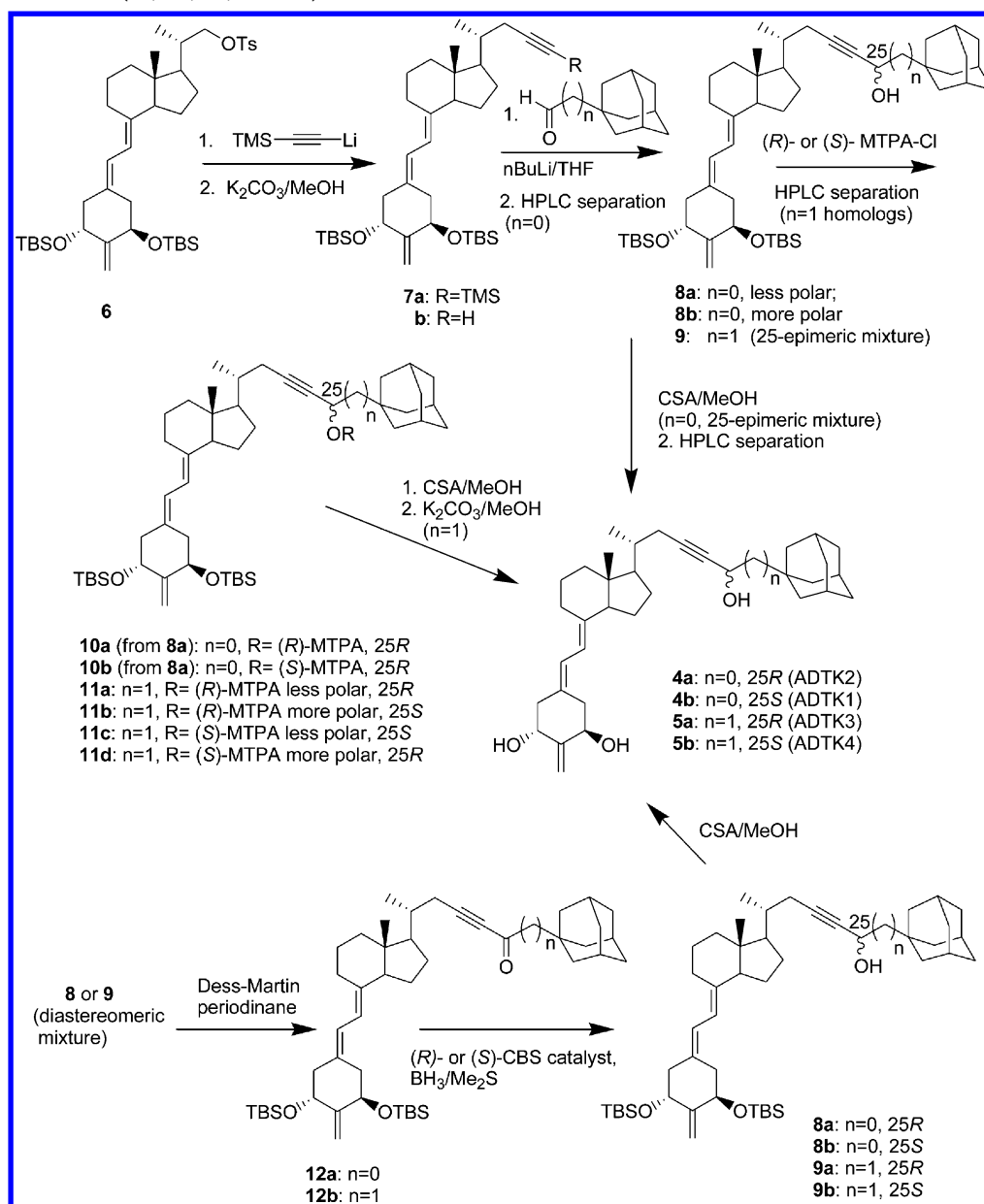
Vitamin D analogues for use as therapeutic agents should not necessarily be super agonist but should have selective activity. We thought that vitamin D compounds that can change the conformation of helix (H) 12 could have antagonist/partial agonist characteristics and may have selective activities. This idea is similar to that for other nuclear receptors such as SERMs¹² and selective progesterone receptor modulators.¹³ The side chain terminal 26-methyl groups of 1,25(OH)₂D₃ interacts with the residues Phe422 and Val418 on H12, and these interactions are thought to be important for its agonistic activity.¹⁴ We have synthesized compounds with a double bond and an adamantane ring on the side chain of vitamin D (2 and 3) (Chart 1).¹⁴ The terminal adamantane ring was expected to clash with the residues on H12, changing the H12 conformation, and the double bond at position 22 was expected to increase the side chain rigidity. The 2-methylene-19-nor A-ring system was selected because it is much more stable to acids, oxidation, irradiation, and heat than the natural triene system of vitamin D is, and it can be synthesized much more readily than normal vitamin D compounds. The 2-methylene-19-nor A-ring system was developed by DeLuca's group and is found in super agonistic compounds such as 2MD.⁹ Our compounds (2 and 3) had significant VDR affinities (2–100% that of 1) and selective VDR modulator activities.¹⁴ However, their efficacies of transcriptional activities were low (<15%): i.e., these compounds 2 and 3 act as antagonists. The need for analogues with higher transactivation efficacies prompted us to synthesize further analogues with more rigidity, i.e., 25- and 26-adamantyl-2-methylene-23,23,24,24-

tetrahydro-19-norvitamin D derivatives (4a,b and 5a,b) (Chart 1). These vitamin D derivatives have significant VDR affinities, partial agonistic activities, and selectivities in the expression of genes in various cell types. The X-ray crystal structures of rVDR-ligand binding domain (LBD) complexed with 4b, 5a, and 5b revealed in part their selective activities.

RESULTS

Synthesis of 25- and 26-Adamantyl-23-yne-19-norvitamin D Compounds ADTK1–4 (4b,a and 5a,b). We synthesized four new 2-methylene-19-norvitamin D derivatives (4a,b and 5a,b) starting from 22-tosylate 6, which was synthesized¹⁴ from D-(–)-quinic acid as an A-ring precursor and vitamin D₂ as a CD-ring plus side chain precursor (Scheme 1). The 22-tosylate 6 was treated with TMS-acetylene (MeLi in dioxane, 105 °C, 80%) and then with K₂CO₃ (THF/MeOH, 95%) to remove the C-TMS group to give acetylene compound 7b. To compound 7b was added nBuLi/THF at 0 °C, and after several minutes the solution was treated with 1-adamantylformaldehyde (n = 0) or 1-adamantylacetaldehyde (n = 1), giving the adamantyl alcohols 8 and 9 in 93% and 80.5%, respectively, as a 1:1 mixture of epimers at C(25). The diastereomeric mixture 8 was separated by HPLC to give less polar 8a and more polar 8b. The diastereomeric mixture 9, which could not be separated by common HPLC columns, was converted to (R)- and (S)-α-methoxy-α-(trifluoromethyl)-phenyl acetic acid esters [(R)- and (S)-MTPA esters, 11a,b and 11c,d, respectively] by treatment with (S)- and (R)-MTPA-Cl (Et₃N, dimethylaminopyridine DMP, CH₂Cl₂, 81% and 41%), respectively, which were readily separated by HPLC. Deprotection (camphor sulfonic acid CSA, MeOH, room temperature) of 8a and 8b yielded the target compounds 4a (ADTK2) (94%) and 4b (ADTK1) (91%), respectively. Similarly, deprotection of 11a and 11d ((1) CSA,

Scheme 1. Resolution and Stereoselective Synthesis of 25- and 26-Adamantyl-2-methylene-22,22,23,23-tetrahydro-19-norvitamin D Derivatives (4a, 4b, 5a, and 5b)



MeOH; (2) K₂CO₃, MeOH) yielded compound **5a** (ADTK3) (56%) and **11b** and **11c** gave **5b** (ADTK4, 67%).

Stereoselective Synthesis of ADTK1–4 (**4b,a** and **5a,b**).

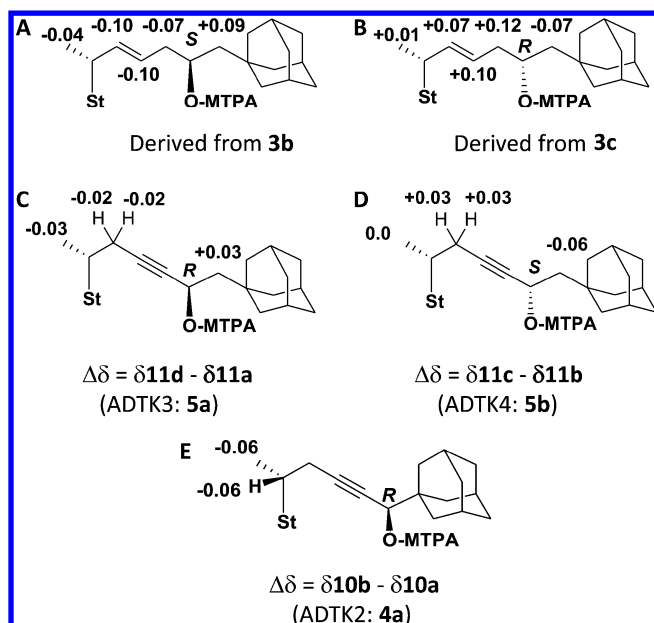
The stereoselective syntheses of **4a,b** and **5a,b** were achieved by reduction of the 25-keto compounds **12a** and **12b** with a chiral oxazaborolidine catalyst.¹⁵ The 25-hydroxyl compounds **8** and **9** were oxidized (Dess–Martin periodinane, DMP) to ketones **12a** (84%) and **12b** (68%), respectively, and selective reduction of the ketones was examined. Among several asymmetric catalysts, B-methyl-4,5,5-triphenyl-1,3,2-oxazaborolidine (BMTO)^{15d} and Corey–Bakshi–Shibata catalyst (CBS),^{15a–c} worked excellently. Reduction of **12a** with the (R)-BMTO catalyst in the presence of BH₃–SMe₂ (THF, 0 °C) gave the 25R-epimer **8a** in 70% yield with 78% de. Reduction of **12a** with the (R)-CBS catalyst (BH₃–SMe₂, THF, 0 °C) gave **8a** more selectively (91% de) in 86% yield. Reduction of **12a** with the (S)-CBS catalyst proceeded similarly to yield the 25S-epimer **8b** (87% de) in 75% yield. The

R- and S-catalysts therefore showed the same stereoselectivities as previously reported.¹⁵ Catalysts with the R-configuration gave the 25R-isomer **8a**, and with S-configuration yielded 25S-isomer **8b** with high selectivities. Selective reduction of **12b** with (R)- and (S)-CBS catalysts yielded **9a** and **9b**, respectively, with high selectivity and in good yields (>95% de, 62% yield and >95% de, 62% yield, respectively).

Determination of C(25) Stereochemistry of ADTK1–4 (4b,a** and **5a,b**) by ¹H NMR Spectroscopy.** We determined the stereochemistry at C(25) of **4a**, **4b**, **5a**, and **5b** by using the new Mosher method.¹⁶ Epimer **8a** of the 25-hydroxy compound was treated with (S)- and (R)-MTPA-chloride to give (R)- and (S)-MTPA esters **10a** and **10b**, respectively. We also obtained pairs of (R)- and (S)-MTPA esters of the 26-adamantyl compound (**11a,b** and **11c,d**, respectively), as described above. We used one- and two-dimensional ¹H NMR spectra to identify the signals from protons in the side chain. The Δδ^S –

δ^R) of the protons on the side chains of three pairs of MTPA esters are shown in Chart 2C,D,E. The $\Delta\delta$ values of H-20 and

Chart 2. Determination of Stereochemistry at C(25) of Adamantyl-19-norvitamin D Derivatives (4a,b and 5a,b) Using the New Mosher Method^a



^a(A,B) Determination of the C(25) stereochemistries of adamantyl Δ^{22} -vitamin D compounds **3b** and **3c** as reported.^{14a} Determination of the C(25) stereochemistries of **11a** and **11d** derived from ADTK3 (**5a**) (C), **11b** and **11c** derived from ADTK4 (**5b**) (D), and **10a** and **10b** derived from ADTK2 (**4a**) (E).

−21 (both −0.06) of **10a** and **10b** were correlated to the 25R-configuration, although the H-22 signals cannot be well assigned. Because the C(25) stereochemistry of **4b** (ADTK1), which was obtained by deprotection of **8b**, was confirmed to be *S* by X-ray crystallographic analysis of the rVDR complex (described below), the stereochemistries of **4a** and **4b** were confirmed to be *R* and *S*, respectively.

As shown above, we confirmed that **11a** (*R*-MTPA-ester) and **11d** (*S*-MTPA-ester) were converted to **5a**, and **11b** (*R*-MTPA-ester) and **11c** (*S*-MTPA-ester) to **5b**. The $\Delta\delta$ values $\delta(11d) - \delta(11a)$ were −0.02, −0.02 (H22), −0.03 (H21), and +0.03 (H26), and accorded with the 25R stereochemistry (Chart 2C). The $\Delta\delta$ values $\delta(11c) - \delta(11b)$ were +0.03 (H22), 0.0 (H21), and −0.06 (H26) and accorded with the 25S stereochemistry (Chart 2D). The stereochemistries of **5a** and **5b** were determined to be *R* and *S*, respectively, by X-ray crystal structural analysis of their rVDR complexes, as described below. All the stereochemistries at C(25) of the synthetic compounds **4a,b** and **5a,b** were therefore successfully determined using the new Mosher method. Chart 2 shows the present results compared with the corresponding results for our double-bond compounds (**3b** and **3c**).^{14a}

Biological Activities of Adamantyl Vitamin D Compounds ADTK1–4 (4b,a and 5a,b). VDR Affinity. The VDR affinities of these vitamin D derivatives (**4a**, **4b**, **5a**, and **5b**) were determined based on competitive binding between [³H]-1,25-(OH)₂D₃ and the substrate using recombinant hVDR-LBD.¹⁷ The results are shown in Figure 1. The 25S-adamantyl compound **4b** had the highest activity, IC₅₀ 0.5 nM, about 90%

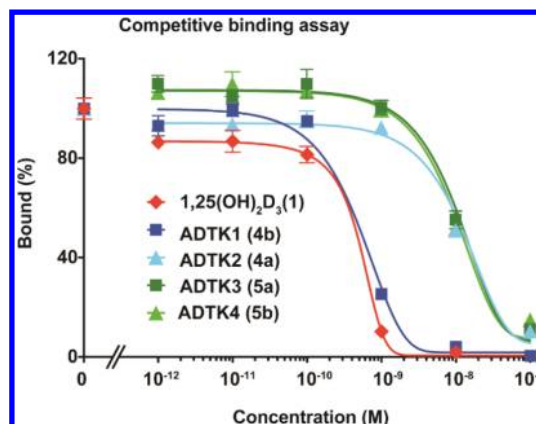


Figure 1. Competitive binding assays of adamantyl-19-norvitamin D derivatives **4a**, **4b**, **5a**, and **5b** compared with 1,25(OH)₂D₃ (**1**). hVDR-LBD expressed as glutathione S-transferase fusion protein was incubated with [³H]-1,25(OH)₂D₃ in the presence of nonradioactive 1,25-(OH)₂D₃ (**1**) (red tilted square), **4a** (blue square), **4b** (cyan triangle), **5a** (green square), and **5b** (light green triangle) at a range of concentrations. All values represent means six standard deviations of triplicate assays.

that of 1,25(OH)₂D₃. The IC₅₀s of 25R-adamantyl (**4a**), 25R- (**5a**), and 25S-adamantyl (**5b**) longer side-chain compounds were 12, 13, and 12 nM, respectively.

Transcriptional Activity. VDR transactivation by ADTK1–4 (**4b,a** and **5a,b**) was evaluated using a luciferase reporter assay in human kidney cell lines (HEK293) transfected with mouse osteopontin vitamin D response elements (VDRE, SPP × 3-tk-LUC) and hVDR (pCMX hVDR) (Figure 2A).^{14d} Compound **4b** had the highest activity (EC₅₀ 0.07 nM, efficacy 81% that of the natural hormone) of the four compounds. The other compounds **4a**, **5a**, and **5b** had similar activities: EC₅₀ (efficacy) **4a** 6.6 nM (38%), **5a** 1.5 nM (70%), and **5b** 1.1 nM (63%). It is worth noting that all the synthetic analogues have partial agonist activities in the transcriptional assay in HEK293 cells (Figure 2A). Their activation efficacies do not exceed that of 1,25-(OH)₂D₃ (**1**), even at doses 100 times higher. These compounds **4a**, **5a**, and **5b**, except for **4b**, inhibited weakly the transactivation induced by the natural hormone **1** (10 nM) (Figure 2B), while antagonist **3a** inhibited dose dependently the action of 1,25(OH)₂D₃.

Mammalian Two-Hybrid Assays. The effects of the adamantyl vitamin D compounds on the binding of VDR to various cofactors were evaluated by mammalian two-hybrid assays in HEK293 cells.¹⁸ In these experiments, the effects of the ligands on VDR-retinoid X receptor α (RXR α) heterodimerization,^{19,20} as well as VDR-coregulator binding including the steroid receptor coactivator 1 (SRC-1; or nuclear receptor coactivator 1 NCoA1),²¹ nuclear receptor corepressor 1 (N-CoR),²² and silencing mediator of retinoic acid and thyroid hormone receptor (SMRT or nuclear receptor corepressor 2, N-CoR2),²³ were evaluated by a luciferase reporter assay.¹⁸ The results are shown in Figure 3.

Binding of VDR to RXR α . Ligand binding promotes heterodimerization of VDR with RXR α , which is essential for the VDR to recognize VDREs in the promoters of the target genes.^{19,20} Adamantyl vitamin D **4b** activates (EC₅₀ 0.6 nM) the VDR to bind to RXR α similarly to 1,25(OH)₂D₃ (EC₅₀ 0.7 nM) (Figure 3A). The other compounds **4a** (EC₅₀ 4.4 nM), **5a** (EC₅₀ 2.3 nM), and **5b** (EC₅₀ 0.8 nM) were a little less active than **4b**

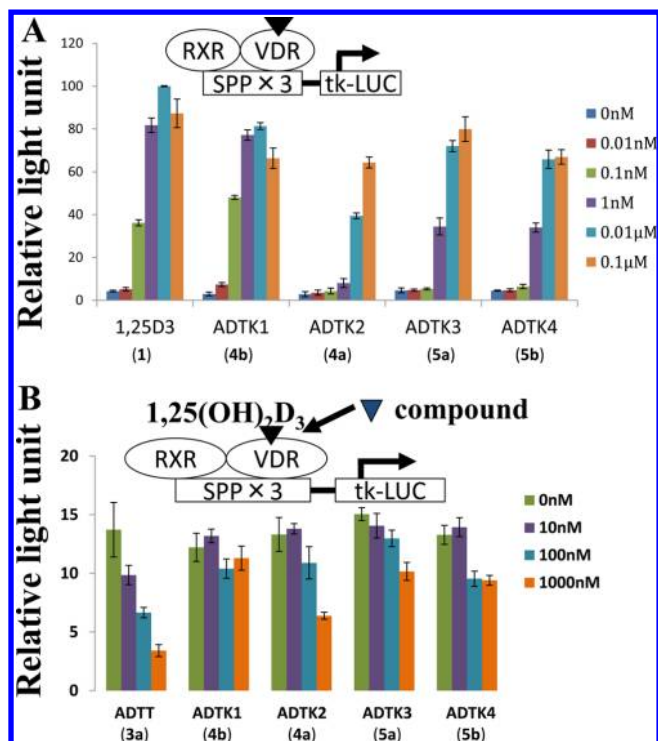


Figure 2. Transactivation of hVDR by adamantly-19-norvitamin D derivatives **4a**, **4b**, **5a**, and **5b** compared with $1,25(\text{OH})_2\text{D}_3$ (**1**). (A) HEK293 cells were cotransfected with TK-Spp \times 3-LUC reporter plasmid and pCMX-VDR, and 8 h after transfection the cells were treated with several concentrations of **4a**, **4b**, **5a**, **5b**, and $1,25(\text{OH})_2\text{D}_3$ (**1**). After 24 h, the cells were harvested for assaying luciferase and β -galactosidase activity using a luminometer (Molecular Devices, Sunnyvale, CA). (B) Antagonistic effect of vitamin D derivatives, **4a**, **4b**, **5a**, **5b**, and ADTT **3a**, on hVDR activated by $1,25(\text{OH})_2\text{D}_3$ (**1**). HEK293 cells were cotransfected as in A and were treated with vitamin D derivatives (**4a**, **4b**, **5a**, **5b**, and **3a**) at a range of concentrations in the presence of $1,25(\text{OH})_2\text{D}_3$ (**1**) (10 nM).

(Figure 3A). These results show that all analogues induce VDR-RXR binding.

Binding of VDR to SRC-1. SRC-1²¹ directly binds to the activation function 2 (AF2) surface of nuclear receptors and stimulates the transcriptional activities in a hormone-dependent manner. This coactivator plays a central role in creating multisubunit coactivator complexes that act by participating in both chromatin remodeling and recruitment of general transcription factors.²¹ The (2S)-adamantly compound **4b** activated the binding of VDR to SRC-1 more strongly (EC_{50} 1.5 nM) than the natural hormone **1** did (EC_{50} 1.9 nM) (Figure 3B). The other compounds **4a** (EC_{50} 15.0 nM), **5a** (EC_{50} 6.5 nM), and **5b** (EC_{50} 13.5 nM) activated the VDR less potently. These results indicate that SRC-1 binds more strongly to the AF-2 surface of the VDR bound **4b** than that bound the natural hormone **1**.

Binding of VDR to N-CoR. N-CoR²² mediates transcriptional repression and, as part of a complex, promotes histone deacetylation and the formation of repressive chromatin structures which may impede the access of basal transcription factors. Thus, **4b** dose-dependently inhibits binding of the VDR to N-CoR (EC_{50} 0.4 nM) slightly more potently than $1,25(\text{OH})_2\text{D}_3$ does (EC_{50} 0.5 nM) (Figure 3C). The other analogues, **4a** (EC_{50} 4.0 nM), **5a** (EC_{50} 3.7 nM), and **5b** (EC_{50} 1.8 nM), inhibited binding of the VDR to N-CoR less potently than **4b**. The ability of adamantly compounds to inhibit the binding of the

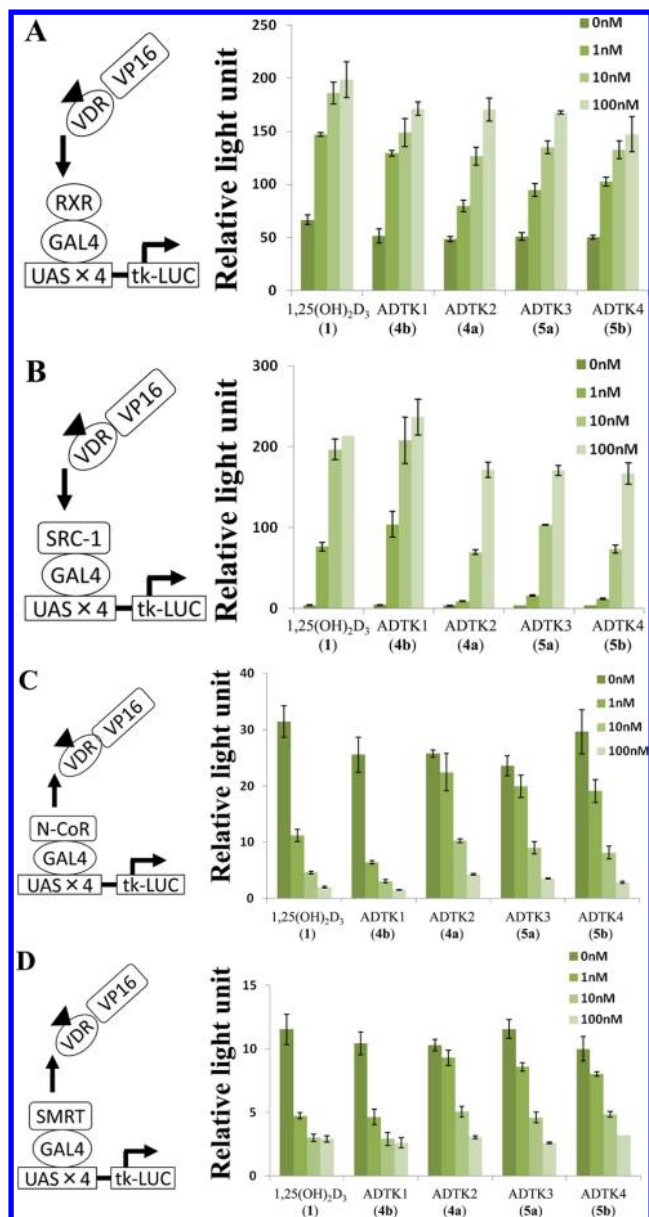


Figure 3. Effect of vitamin D derivatives **4a**, **4b**, **5a**, and **5b** on coactivator recruitment in a mammalian two-hybrid assay. (A) Effects of vitamin D derivatives on interaction between VDR and RXR α . HEK293 cells were cotransfected with CMX-GAL4-RXR α , CMX-VP16-VDR, and MH100(UAS) \times 4-tk-LUC and treated with vitamin D compounds **4a**, **4b**, **5a**, **5b**, or $1,25(\text{OH})_2\text{D}_3$ (**1**) at a range of concentrations. (B) Effects on interactions between VDR and SRC-1. HEK293 cells were cotransfected with CMX-GAL4-SRC-1, CMX-VP16-VDR, and MH100(UAS) \times 4-tk-LUC and were treated with vitamin D compounds **4a**, **4b**, **5a**, **5b**, or $1,25(\text{OH})_2\text{D}_3$ (**1**) at a range of concentrations. Effects on interactions of VDR with NCoR-1 (C) or SMRT (D). HEK293 cells were cotransfected with CMX-GAL4-N-CoR or CMX-GAL4-SMRT in combination with CMX-VP16-VDR and MH100(UAS) \times 4-tk-LUC and were treated with vitamin D derivatives **4a**, **4b**, **5a**, **5b**, or $1,25(\text{OH})_2\text{D}_3$ (**1**) at a range of concentrations.

two proteins is inversely proportional to the ability to activate binding of the VDR to SRC-1.

Binding of VDR to SMRT (NCoR2). The effect of **4b** (EC_{50} 0.5 nM) in inhibiting binding of the VDR to SMRT²³ was slightly less potent than that of $1,25(\text{OH})_2\text{D}_3$ (EC_{50} 0.4 nM). Other analogues inhibited the binding of SMRT to the VDR less

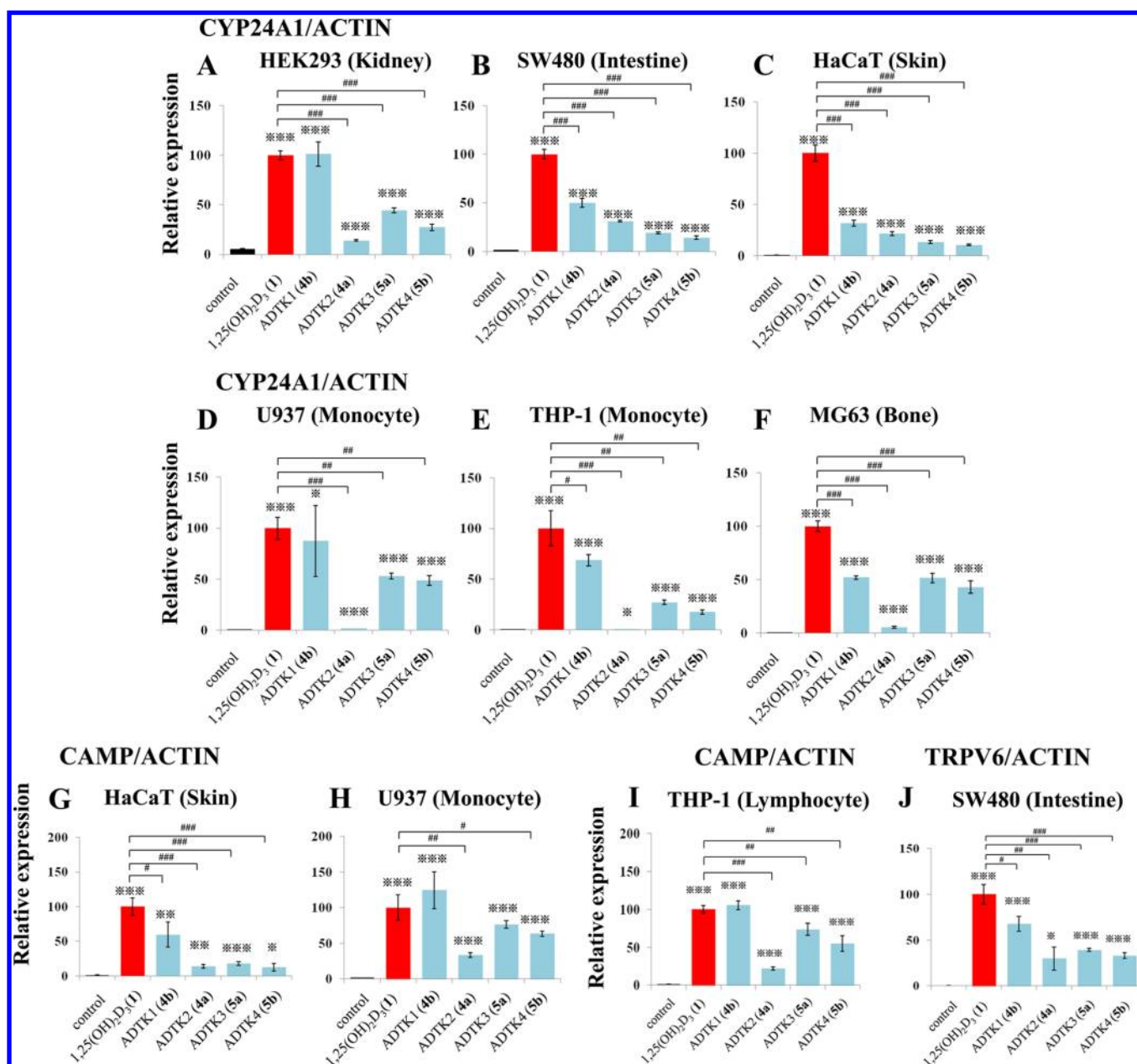


Figure 4. Effects of vitamin D derivatives **4a**, **4b**, **5a**, and **5b** on expression of *CYP24A1* gene in kidney derived HEK293 (A), intestinal SW480 (B), keratinocyte HaCaT cells (C), monocyte-derived U937 (D), monocyte-derived THP-1 (E), and bone-derived MG63 (F) cells. Effects on the expression of *CAMP* gene in HaCaT (G), U937 (H), and THP-1 cells (I), and of *TRPV6* gene in SW480 cells (J). Cells were treated with each sample (100 nM) for 24 h. *, $p < 0.05$; **, $p < 0.01$; ***, $p < 0.001$.

potently than **4b**: **4a** (EC_{50} 4.1 nM), **5a** (EC_{50} 2.4 nM), and **5b** (EC_{50} 2.8 nM) (Figure 3D).

Effect of Adamantyl Vitamin D Analogues on Endogenous Gene Expression in Various Cells. To examine the tissue-selective action of analogues **4a,b** and **5a,b**, we evaluated the expression of *CYP24A1*²⁴ gene in kidney-epithelium-derived HEK293, intestinal-mucosa-derived SW480, osteoblast-derived MG63, myeloid-derived THP-1 and U937, and skin-keratinocyte-derived HaCaT cells. We also examined the effect of the analogues on the expression of other genes, such as cathelicidin antimicrobial peptides (*CAMP*)²⁵ in THP-1, U937, and HaCaT cells, and transient receptor potential vanilloid 6 (*TRPV6*)²⁶ in SW480 cells. In all the experiments, we used equal concentrations (100 nM) of the ligands (**1**, **3a,b**, and **4a,b**).

CYP24A1. *CYP24A1* is an enzyme²⁴ that inactivates 1,25-(OH)₂D₃ and its precursor 25-hydroxyvitamin D₃ (25-OHD₃) by hydroxylating their 24-position to yield the corresponding 24-hydroxylated metabolites. Binding of the ligands to the VDR induces enzyme expression in all the target tissues. The 25S-adamantyl compound **4b** induced *CYP24A1* mRNA expression in HEK293 cells similarly to the natural hormone (Figure 4A). The other compounds, **4a**, **5a**, and **5b**, increased *Cyp24A1* mRNA expression by 15%, 45%, and 30% of the activity of the natural hormone.

Interestingly, cell-type-selective gene induction was observed. In intestinal SW480 and in bone MG63 cells, **4b** activated the *CYP24A1* gene with about 50% of the activity of the natural hormone (Figure 4B,F). In skin HaCaT cell, mRNA expression of *CYP24A1* was 30% (Figure 3C) and in blood U937 and THP-

Table 1. Data Collection and Refinement Statistics

ligand	ADTK1 (4b)	ADTK3 (5a)	ADTK4 (5b)
PDB ID	3VTB	3VTC	3VTD
X-ray source	KEK-PF BL-5A	KEK-PF BL-5A	KEK-PFAR NW12A
space group	C2	C2	C2
cell dimensions			
<i>a, b, c</i> (Å)	153.56, 43.20, 42.49	126.85, 45.73, 46.64	153.18, 43.90, 42.53
α, β, γ (deg)	90.00, 95.56, 90.00	90.00, 93.87, 90.00	90.00, 95.73, 90.00
resolution range (Å)	50.00–2.00	50.00–1.50	50.00–2.70
(outer shell)	(2.07–2.00)	(1.55–1.50)	(2.80–2.70)
no. of reflections	66943	147172	29041
unique reflections	19 104	43 106	7900
completeness (%)	97.3	96.8	98.6
(outer shell)	(99.9)	(83.3)	(99.0)
R_{merge}	0.042	0.041	0.061
(outer shell)	(0.249)	(0.182)	(0.311)
Refinement Statistics			
resolution range (Å)	50.00–2.00	50.00–1.50	50.00–2.70
(outer shell)	(2.07–2.00)	(1.55–1.50)	(2.80–2.70)
R factor $R_{\text{free}}/R_{\text{work}}$	0.286/0.246	0.209/0.184	0.278/0.213
(outer shell)	(0.506/0.521)	(0.237/0.206)	(0.400/0.325)

1 cells, 70–90% that of the natural hormone (Figures 3D,E). The 25R-isomer **4a** showed a low but clearer cell type dependent activity differences: in U937 and THP-1 cells 1%, MG63 5%, HEK293 14%, HaCaT cells 22%, and SW480 32%. The longer side chain compounds **5a** and **5b** showed about 50% activity in bone (MG63) and monocyte (U937) cells but showed lower activities (10–30%) in monocyte (THP1), intestine (SW480), and skin (HaCaT) cells (Figure 4). These adamantyl compounds (**4a,b** and **5a,b**) therefore all have different tissue selectivities.

Cathelicidine Antimicrobial Peptide (CAMP). CAMP²⁵ is an innate antimicrobial peptide and its induction has been observed, for example, in myeloid cells, keratinocyte, and intestinal cell lines. The expressions of the CAMP gene by **4b** in the monocytic cell lines U937 and THP-1 and in keratinocyte HaCaT cells were increased compared with those of CYP24A1 (85%, 70%, and 30%, respectively) to 125%, 105%, and 60%, respectively (Figure 4H,I,G). The 25-epimer **4a** showed lower activities in U937, THP-1, and HaCaT cells, 30%, 20%, and 15%, respectively. The longer homologues **5a** and **5b** had moderate activities in U937 cells, 75% and 65%, respectively, and in THP-1 cells 74% and 55%, respectively (Figure 4H,I). However, they showed much lower activities in HaCaT cells, 20% and 15%. Thus, **5a** and **5b** showed 3.5–4-fold higher activities in monocytic cells than in skin cells (Figure 4G).

Transient Receptor Potential Vanilloid 6 (TRPV6). TRPV6²⁶ is a membrane calcium channel that is responsible for the first step in calcium absorption in the intestine. Its expression by **4b** in intestinal SW480 cells (Figure 4J) was similar (65%) to the expression of the CYP24A1 gene. The longer homologues **5a** and **5b** induced TRPV6 expression less strongly (40% and 35%, respectively) but twice as strongly as the CYP24A1 gene. The activities of **4a** were similar (30%) for TRPV6 and CYP24A1.

X-ray Crystal Structural Analysis of rVDR-LBD Complexed with ADTK1, ADTK3, and ADTK4 (4b, 5a, and 5b). X-ray crystallographic structural analyses are essential for investigating the structure–activity relationships of the target compounds (**4a,b** and **5a,b**). The rVDR-LBD bound to **4b**, **5a**, and **5b** were crystallized as ternary complexes with a peptide containing LXXLL motif derived from VDR-interacting protein complex component DRIP205 (or MED1)²⁷ and analyzed to

resolutions of 2.0, 1.5, and 2.7 Å, respectively (Table 1). The complex with **4a** (ADTK2) was also crystallized, but it was unstable to achieve good resolution (Supporting Information Figure S1, Table S1, and crystal data of rVDR-LBD/4a/DRIP). All of the complexes belonged to the space group C2. The root-mean-square deviations (rmsd) of the C α atoms of the rVDR-LBDs complexed with **4b**, **5a**, and **5b** compared with the 1,25(OH)₂D₃ complex (2ZLC)^{28a} were 0.32, 0.56, and 0.38 Å, respectively. The complex with **5a** had the largest rmsd and was found to have somewhat a different unit cell structure (Supporting Information Figure S2) from the others, such as complexes with **4b** and **1** (2ZLC). Why does the complex with **5a** have a different unit cell structure? First, this might be a result of the positioning of the 25-hydroxyl group of **5a**. As shown in the overlay of the rVDR LBDs complexed with **5a** and **1** (2ZLC) (Figure 5A), the 25-hydroxyl group of **5a** takes a different position, which overlaps with the His393 of the complexes with **1**. Then the torsion angle (N–C α –C β –C γ) of His393 was changed significantly, from 170.7° of the complex with **1** to –72.1° of the complex with **5a**, which then caused the C α positional changes of Thr302 (1.4 Å), Leu303 (2.5 Å), Glu304 (3.1 Å), and Leu305 (2.4 Å), as shown in Figure 5B. Interestingly, in **5b** complex, the positional shifts of Thr302 (1.1), Leu303 (0.7 Å), Glu304 (0.9 Å), and Leu305 (1.0 Å) are not as large as those of **5a** complex, and Leu303 and Glu304 are situated similarly to those of the complex with **1** (Figure 5C). In the VDR/4b complex, Leu303 and Glu304 interact with Ile134 (3.7 Å) and His130 (2.7 Å), respectively, of another VDR in the neighboring crystal unit (Supporting Information Figure S3A); this would stabilize the crystal packing. However, in the complex with **5a**, similar intercrystal-unit interactions are impossible because of the significant positional shifts of these residues (Supporting Information Figure S3B). In the complex with **5b**, the two residues, Leu303 and Glu304, are positioned similarly to **4b** and **1** rather than **5a** (Supporting Information Figure S3B).

The rVDR complexes of the ligands **4b**, **5a**, and **5b** all adopted the canonical active conformation (Supporting Information Figure S4). The side chain of the all ligands in the VDR adopted similar 16,17,20,22 dihedral angles directed toward the 21-methyl group of the natural hormone (Figure 5A,C): the

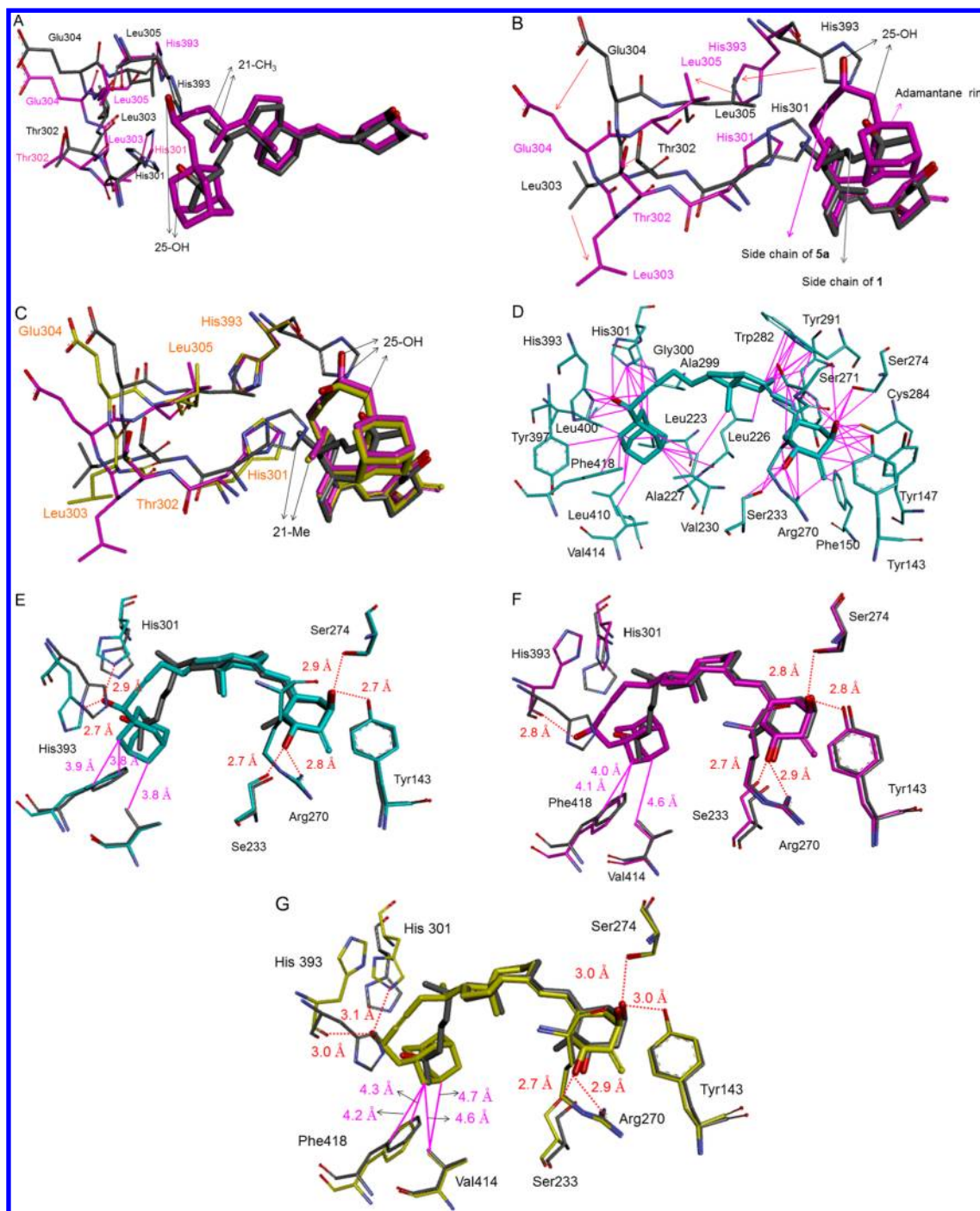


Figure 5. X-ray crystal structures of rVDR-LBD complexed with vitamin D compounds **4b**, **5a**, and **5b**. (A) Overlay of rVDR-LBD complexes with **5a** (magenta) and **1** (atom type). Residues His393 and His301-Leu305 are shown with narrow sticks. This view is shown focusing on the ligand structures. (B) Different view of the structures shown in (A) focusing on the residues His393 and His301-Leu305. (C) Overlay of rVDR-LBD complexes with **5a** (magenta), **5b** (yellow), and **1** (atom type). Residues His393 and His301-Leu305 are shown with the same color as the ligand. (D) van der Waals interactions (magenta line) of **4b** (atom type) with VDR residues (atom type) within 4 Å distance from **4b**. (E) Overlay of rVDR-LBD complexes with **4b** (cyan) and **1** (atom type). Hydrogen bonding interactions (red dotted lines) and van der Waals interactions with H12 residues (magenta) are shown. (F) Overlay of rVDR-LBD complexes with **5a** (magenta) and **1** (atom type). Hydrogen bonding interactions (red dotted line) and van der Waals interactions (magenta line) with H12 residues are shown. (G) Overlay of rVDR-LBD complexes with **5b** (yellow) and **1** (atom type). Hydrogen bonding interactions and van der Waals interactions with H12 residues are shown.

16,17,20,22-torsion angles of **4b**, **5a**, and **5b** were 54.5, 53.0, and 48.6°, respectively, whereas that of 1,25(OH)₂D₃ was -44.3° and 16,17,20,21 dihedral angle was 77.2°. In these conformations, the terminal adamantane rings of **4b**, **5a**, and **5b** are placed around the 26,27-dimethyl group of **1**, and the other parts of the

side chains occupy different positions from those in the natural hormone (Figure 5A,B,C).

The adamantane ring of **4b** interacts with as many as 10 residues within 4 Å, i.e., Leu223, Leu226, Ala227, and Val230 (H3), His301 (loop 6–7), Tyr397 and Leu400 (H11), Leu410

(loop11–12), and Val414 and Phe418 (H12) (Figure 5D). Most importantly, Phe418 and Val414 of **4b** have closer contacts with the adamantane ring (both 3.8 Å) than the 26-methyl group of 1,25(OH)₂D₃ (**1**) in all known VDR-LBD complexes: rat (both 4.3 Å), human (4.0 and 4.3 Å, respectively), and zebra fish (4.4 and 4.1 Å, respectively). Ligand **4b** in the VDR forms hydrogen bonds (2.7–2.9 Å) with the same six residues as the natural hormone (Figure 5E), but His301 and 393 adopt different conformations compared with the 1,25(OH)₂D₃ complex (Figure 5E), although the C α positional shifts are not large (0.6 and 0.4 Å, respectively). The methylene group at C(2) of **4b** interacts with Tyr143 (3.8 Å), Arg270 (3.5 Å), and Phe150 (4.0 Å) as does 2MD (Figure 5D). Phe418 in the complex of **4b** forms CH– π bonds with His393. All these data accord with **4b** having a high VDR affinity.

The complex of C(25) epimer **4a** forms normal hydrogen bonds with Arg270 (2.8 Å), Ser274 (2.8 Å), and His393 (2.5 Å), weak hydrogen bonds with Trp143 (3.1 Å) and Ser233 (3.2 Å), and no hydrogen bond with His301 (4.6 Å) (Supporting Information Figure S1). The VDR therefore anchors **4a** more weakly than **4b**.

The complex with **5a** has the largest positional shifts at 301–306 (rmsd 1.8 Å) compared with the 1,25(OH)₂D₃ complex (2ZLC) (Figure 5B). It was also noted that the positioning of DRIP peptide differs significantly (at the LXXLL part, rmsd 0.8 Å). The two A-ring hydroxyl groups form hydrogen bonds with Ser233, Arg270, Tyr143, and Ser274 (2.7–2.9 Å) (Figure 5F). The 25-hydroxyl group does not form hydrogen bond with the imidazole nitrogen of His393 but does with its main chain carbonyl group (2.8 Å); it forms no hydrogen bond with His301. The methylene group at C(2) interacts with the same residues Tyr143 (3.9 Å), Arg270 (3.5 Å), and Phe150 (4.0 Å) as **4b** does.

In the complex with rVDR-LBD, **5b** interacts similarly to **5a** except around C25. The 25-hydroxyl group forms weak hydrogen bonds with the imidazole nitrogen of His301 (3.1 Å) and the main chain carbonyl of His393 (3.0 Å) (Figure 5G). The C(2) methylene group of **5b** interacts differently from that of **5a** and 2MD: in addition to Tyr143 (3.9 Å), Arg270 (3.5 Å), and Phe150 (4.0 Å), Ser233 (3.9 Å) interacts with the CH₂ at a closer distance than that of **5a** complex (4.2 Å). Here, the difference in the side chain structure affects the conformations around the A ring too.

DISCUSSION

We have previously determined the crystal structures of the complex of rVDR bound to an antagonist/partial agonist **3a** (ADTT) [VDR affinity 80% of the natural hormone (**1**), transactivation EC₅₀ 10^{−9} M (15% efficacy), inhibition of the transactivation of **1** (IC₅₀ 3 × 10^{−9} M)] and the DRIP peptide. However, the VDR/**3a** complex adopts the active conformation.^{14c} The rVDR complex with the one-carbon-longer analogue **3e** (ADMI4) [1/20 relative VDR affinity, transactivation EC₅₀ 2.4 × 10^{−8} M (less than 10% efficacy), inhibition of the transactivation of **1** IC₅₀ 3 × 10^{−8} M] also adopts the active form.^{14c} We thus confirmed that rVDR complexed with antagonists can adopt the active conformation in the crystal structure in the presence of the DRIP peptide. We assumed that the DRIP peptide trapped the active conformation that exists as a minor conformation in solution (assuming 10–15% on the basis of the transactivation efficacy) by binding to its AF2 surface.

It is therefore not strange that the crystal structures of the rVDR-LBDs bound to the partial agonists **4b**, **5a**, and **5b** adopt the active conformations. The adamantane ring in all these

compounds faces H12 (Figure 6A). We analyzed the interactions between the residues Phe418 and Val414 on H12 and the

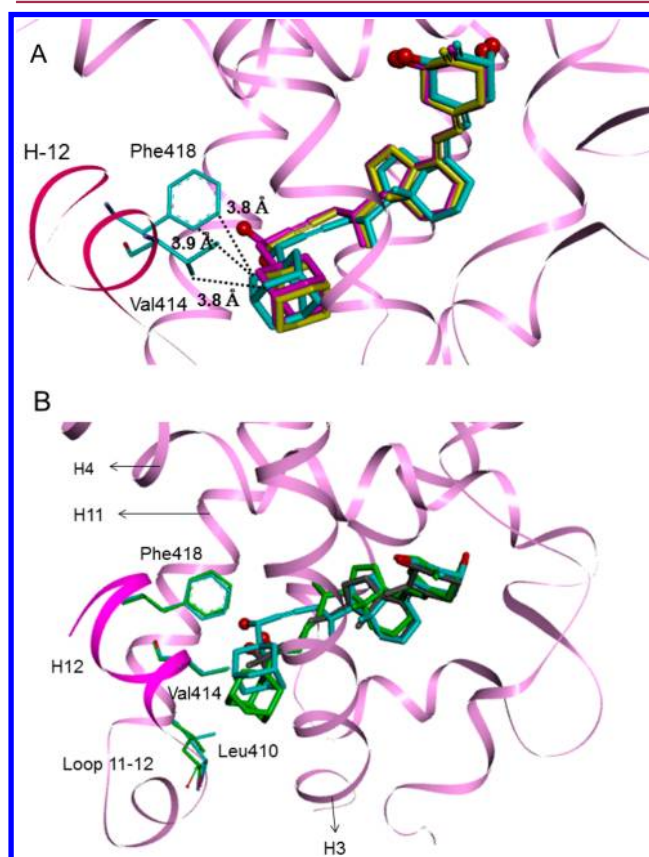


Figure 6. Interactions of adamantane ring with H12 residues in the rVDR-LBD complexes. (A) Overlay of rVDR complexes of **4b** (cyan), **5a** (magenta), and **5b** (yellow). The protein of **4b** complex is shown with pink ribbon with H12 magenta. Interaction of **4b** with the H12 residues, Phe418 and Val414, are shown with black dotted lines. The interactions of other ligands with H12 residues are shown in Table 2. (B) Overlay of the complexes with partial agonist **4b** (cyan), antagonist **3a** (green), and natural hormone **1** (atom type). The protein of **4b** complex is shown with a pink ribbon with H12 in magenta and three residues, Phe418, Val414 and Leu410, interacting with the adamantane ring of the ligands are shown.

adamantane ring of the ligands (**4a**, **5a**, and **5b**) in detail and compared them with those of other known VDR ligands (Table 2). It seems that H12 binds more tightly to the adamantane ring of **4b** than the 26-methyl group of 1,25(OH)₂D₃, as shown by the distance between the two residues and side chain terminals of the ligands (Table 2). The distances between Phe418(422) and Val414(418) and 1,25(OH)₂D₃ are equal to or longer than 4 Å in humans,^{28c} rats,^{28a,b} and zebrafish.^{28d} The side chain terminal of the super agonist KH1060,^{28e} which has a long side chain, is also in a similar region (Table 2, entry 10; Chart 1). However, the adamantane rings of ADTK1 (both 3.8 Å) and antagonist ADMI4 (3.5 and 4.0 Å) are at closer positions (Table 2). According to the equilibrium theory between active and inactive conformations,^{14c,29} we assume that in solution these complexes would shift to an inactive form. It was reported for the zVDR complexes of 26,27-hexafluoro analogue CD578 (Chart 1; entry 13, Table 2) that the terminal fluorine atoms of the ligand are very close to Phe448 (3.6 Å), Val444 (3.5 Å), and Leu440 (3.3 Å), and these close interactions are correlated with the high potency of the

Table 2. Distances (Å) between H12 Residues with the Ligands in VDR

entry	VDR/ligand complexes (PDB code no.)	Phe418 (r), ^a 422 (h), ^b 448, (z) ^c	Val414 (r), 418 (h), 444 (z)
1	rVDR ADTK1 (4b) (3VTB)	3.8, 3.9	3.8
2	rVDR ADTK3 (5a) (3VTC)	4.0	4.60
3	rVDR ADTK4 (5b) (3VTD)	4.2, 4.3	4.8
4	rVDR ADTT (3a) (2ZMI) ^{14c}	4.5	4.3
5	rVDR ADMI4 (3e) (2ZMJ) ^{14c}	3.5	4.0
6	rVDR ADNY (3f) (2ZMH) ^{14c}	4.1, 4.2	4.4
7	rVDR-LBD/1,25(OH) ₂ D ₃ (2ZLC) ^{28a}	4.3	4.3
8	hVDR-LBD/1,25(OH) ₂ D ₃ (1DB1) ^{28c}	4.3	4.0
9	zVDR-LBD/1,25(OH) ₂ D ₃ (2HC4) ^{28d}	4.4	4.1
10	hVDR-LBD/KH1060 (1IE8) ^{28e}	4.4	4.4, 4.0, 4.3
11	rVDR-LBD/2MD (1RJK) ^{28b}	4.1, 4.2	4.5
12	zVDR-LBD/CDS78 (3DR1) ^{28f}	3.5	3.6

^aRat. ^bHuman. ^cZebrafish.

compound. However, these fluorine atoms interact directly with Phe422, with no intervening hydrogen atom. The F–C distance should be compared with (C)H–C distance, which is at least 1 Å shorter (3.0–3.3 Å) than the C(H)–C distance (4.0–4.3 Å). The positioning of the adamantane ring of **4b** is different from that of the double bond analogue **3a**, an antagonist, as shown in the VDR complexes (Figure 6B). The adamantane ring of **3a** in the VDR complex moves to the bottom of the protein to avoid crowding with Phe418 and Val414 on H12. Furthermore, in the VDR, the vitamin D derivatives (**4** and **5**) with an adamantane ring and a triple bond have different side chain structures from those in the natural hormone (Figures 5A,B,C,E,F,G and 6B); this might be one reason why these compounds show different selectivities compared with the natural hormone.

CONCLUSIONS

Newly synthesized adamantyl vitamin D analogues (**4a,b** and **5a,b**) with a triple bond on the side chain are shown to be partial agonists. The adamantane rings of all the compounds face H12 and interact with Phe418 and Val414; furthermore, the side chain positioning differs significantly from that of the natural hormone (Figures 5A–C). The biological potencies of all the analogues are significantly high in terms of VDR affinity and transactivation (Figures 1 and 2). These compounds show significant selectivity in gene expressions in various cell types (Figure 4); for example, the activities of **4b** (ADTK1) in CYP24A1 gene expression in kidney, intestine, and bone were 1, 1/2, and 1/3, respectively, compared with the natural hormone. Similarly, CYP24A1 gene expressions of **5a** (ADTK3) in kidney, bone, and monocyte (U937) were significant for about 50% of the natural hormone but weak in skin (13%) and intestinal (19%) cells. ADTK2 (**4a**) showed selectivity in the expression of different genes; it showed no activity in the expression of CYP24A1 in monocyte U937 and THP-1 cells, but showed significant activities, 33% and 22%, respectively, in the expression of the CAMP gene in the same cells. The side chain structural differences between the 23-ynadamantyl vitamin D compounds (**4b** and **5a,b**) and the natural hormone (Figures 5A–C) may be a reason why the former

compounds showed significant cell-type selectivity. We are investigating further activities in in vivo expressions of various genes and also the effects on the elevation of calcium concentration and bone mineralization.

EXPERIMENTAL SECTION

Chemistry. All nonaqueous reactions were carried out under argon atmosphere in freshly distilled anhydrous solvents. We conducted high-pressure liquid chromatography (HPLC) by using Jasco PU-980 intelligent pumps equipped with an 801-SC solvent programmer and a Jasco UV-970 detector. All samples for biological assays were purified by HPLC and shown to have a purity of >95%. Columns used are YMC-Pack ODS-AM SH-342-5 (10 × 250 mm) or CHIRALPACK IE (4.6 mm × 250 mm). Nuclear magnetic resonance spectra were recorded in CDCl₃ solution on a Bruker Ultra Shield 400 MHz spectrometer (400 MHz for ¹H NMR and 100 MHz for ¹³C NMR). Coupling constants are reported in hertz (Hz). Abbreviations used are singlet (s), doublet (d), triplet (t), quartet (q), and multiplet (m). Low-resolution mass spectra (MS) were obtained by electronic ionization on a Shimadzu GCMSQP-2010NC PLUS 100 spectrometer at 70 eV, and *m/z* values are given with relative intensities in parentheses. High resolution mass spectra (HRMS) were obtained by JEOL JMS-T100LP with DART (direct analysis in real time). Ultraviolet spectra were recorded on a Hitachi U-3300 spectrometer.

1 α -Hydroxy-2-methylidene-24-trimethylsilyl-23,23,24,24-tetradecahydro-19,25,26,27-tetranorvitamin D₃ 1,3-Bis(*tert*-butyldimethylsilyl) Ether (7a**).** To a solution of trimethylsilylacetylene (282 μ L, 2.03 mmol, 3 equiv) in anhydrous dioxane (3.0 mL) at 0 °C was added a 3.0 M hexane solution of MeLi (678 μ L, 2.03 mmol, 3 equiv). The mixture was stirred at 0 °C for 30 min. To this mixture was added a dioxane (3.0 mL) solution of tosylate **6** (494.1 mg, 0.678 mmol), and then the mixture was heated in a sealed tube at 105 °C for 15 h. The reaction mixture was cooled to room temperature, a saturated NH₄Cl solution was added, and the mixture was extracted with ethyl acetate. The organic layer was washed with saline, dried over MgSO₄, and evaporated. The residue was chromatographed on silica gel (54 g) and eluted with 3% ethyl acetate/hexane to give **7a** (356.6 mg, 80%). **7a**: ¹H NMR (CDCl₃) δ 0.02, 0.05, 0.06, 0.08 (each 3 H, s, OSiMe), 0.16 (9 H, s, CSiMe₃), 0.56 (3 H, s, 18-Me), 0.86, 0.90 (each 9H, s, SiBu¹), 1.09 (3H, d, *J* = 6.4 Hz, 21-Me), 4.41–4.45 (2H, m, H-1 and -3), 4.92, 4.97 (each 1H, s, C=CH₂), 5.84 (1H, d, *J* = 11.2 Hz, H-7), 6.21 (1H, d, *J* = 11.2 Hz, H-6). MS (EI) *m/z* (%): 654 (M⁺, 2), 522 (30), 450 (10), 366 (10), 234 (10), 73 (100).

1 α -Hydroxy-2-methylidene-23,23,24,24-tetradecahydro-19,25,26,27-tetranorvitamin D₃ 1,3-Bis(*tert*-butyldimethylsilyl) ether (7b**).** To a solution of **7a** (27.0 mg, 0.041 mmol) in THF/MeOH (1:0.7, 1 mL) was added K₂CO₃ (28.5 mg, 0.21 mmol, 5 equiv), and the mixture was stirred at room temperature for 24 h. After addition of a saturated solution of NH₄Cl, the mixture was extracted with ethyl acetate. The extract was washed with saline, dried over MgSO₄, and evaporated. The residue was chromatographed on silica gel (6.8 g) and eluted with 1% ethyl acetate/hexane to give **7b** (22.8 mg, 95%). **7b**: ¹H NMR (CDCl₃) δ 0.02, 0.06, 0.07, 0.08 (each 3 H, s, SiMe), 0.56 (3 H, s, 18-Me), 0.86, 0.90 (each 9 H, s, *t*-Bu), 1.09 (3 H, d, *J* = 6.4 Hz, 21-Me), 1.95 (1H, t, *J* = 2.4 Hz, terminal acetylene H), 4.41–4.45 (2 H, m, H-1 and -3), 4.92, 4.97 (each 1 H, s, C=CH₂), 5.84 (1 H, d, *J* = 11.2 Hz, H-7), 6.21 (1 H, d, *J* = 11.2 Hz, H-6). ¹³C NMR (CDCl₃) δ -4.90, -4.86, 12.17, 18.16, 18.24, 19.09, 22.18, 23.36, 25.60, 25.78, 25.84, 27.53, 28.69, 30.90, 35.65, 38.58, 40.35, 45.58, 45.62, 47.62, 55.33, 56.16, 69.17, 71.63, 72.52, 83.36, 106.28, 116.25, 122.35, 132.91, 140.87, 152.96. MS (EI) *m/z* (%): 582 (M⁺, 2), 450 (65), 366 (18), 351 (10), 234 (18), 73 (100). HRMS (DART) *m/z* calcd for C₃₆H₆₃O₃Si₂ (M⁺ + OH) 599.432, found 599.427.

25-(1-Adamantyl)-1 α ,25-dihydroxy-2-methylidene-23,23,24,24-tetradecahydro-19,26,27-trinorvitamin D₃ 1,3-Bis(*tert*-butyldimethylsilyl) Ether (8**).** A 1.65 M hexane solution of *n*-BuLi (86 μ L, 0.14 mmol, 2 equiv) was added to a solution of acetylene compound **7b** (41.0 mg, 0.07 mmol) at 0 °C, and 7 min later a solution of 1-adamantylformaldehyde (34.7 mg, 0.21 mmol, 3 equiv) in THF

(420 μL) was added. The mixture was stirred at 0 °C for 2 h, and then saturated NH_4Cl solution was added. The mixture was extracted with ethyl acetate, washed with saline, dried over MgSO_4 , and evaporated. The residue was chromatographed on silica gel (4.7 g) and eluted with 5% ethyl acetate/hexane to give **8** (48.8 mg, 93%) as a mixture of diastereomers at C-25. The mixture was separated by HPLC [Hibar RT LiChrosorb Si 60 (7 μm), 10 mm \times 250 mm, CH_2Cl_2 /hexane 2/3, 4.0 mL/min] to give less polar **8a** and more polar **8b**. **8a** (more polar): $^1\text{H NMR}$ (CDCl_3) δ 0.02, 0.05, 0.06, 0.08 (each 3H, s, SiMe), 0.56 (3H, s, 18-Me), 0.86, 0.90 (each 9H, s, SiBu⁺), 1.11 (3H, d, J = 6.4 Hz, 21-Me), 3.86 (1 H, s, H-25), 4.41–4.45 (2H, m, H-1 and -3), 4.92, 4.97 (each 1H, s, C=CH₂), 5.84 (1H, d, J = 11.2 Hz, H-7), 6.21 (1H, d, J = 11.2 Hz, H-6). MS m/z (%): 746 (M^+ , 2), 614 (18), 596 (20), 366 (20), 234 (12), 135 (100), 73 (80). **8b** (less polar): $^1\text{H NMR}$ (CDCl_3) δ 0.02, 0.05, 0.07, 0.08 (each 3H, s, SiMe), 0.56 (3H, s, 18-Me), 0.86, 0.90 (each 9H, s, SiBu⁺), 1.10 (3H, d, J = 2.4 Hz, 21-Me), 3.86 (1 H, s, H-25), 4.41–4.45 (2H, m, H-1 and -3), 4.92, 4.97 (each 1H, s, C=CH₂), 5.84 (1H, d, J = 11.2 Hz, H-7), 6.21 (1H, d, J = 11.2 Hz, H-6). MS m/z (%): 746 (M^+ , 2), 614 (18), 596 (20), 366 (20), 234 (12), 135 (100), 73 (80).

26-(1-Adamantyl)-1 α ,25-dihydroxy-2-methylidene-23,23,24,24-tetrahydro-19, 27-dinorvitamin D₃ 1,3-Bis(tert-butylidimethylsilyl) Ether (9). Similarly, one-carbon longer homologue **9** was synthesized from **7b** (6.4 mg, 0.011 mmol) and 1-adamantylacetaldehyde (5.88 mg, 0.033 mmol, 3 equiv). After chromatography on silica gel (1.1 g) with 1% ethyl acetate/hexane, **9** (5.3 mg, 80.4%) was obtained as a 1:1 mixture of C-25 epimers. **9**: $^1\text{H NMR}$ (CDCl_3) δ 0.02, 0.05, 0.06, 0.08 (each 3 H, s, SiMe), 0.55 (3 H, s, 18-Me), 0.86, 0.90 (each 9 H, s, SiBu⁺), 1.06 (3 H, d, J = 8.0 Hz, 21-Me), 4.41–4.45 (2 H, m, H-1 and -3), 4.51 (1 H, m, 25-H), 4.92, 4.97 (each 1 H, s, C=CH₂), 5.84 (1 H, d, J = 11.2 Hz, H-7), 6.21 (1 H, d, J = 11.2 Hz, H-6). MS m/z (%): 760 (M^+ , 2), 610 (16), 475 (18), 366 (20), 234 (12), 135 (100), 73 (75).

25R-(1-Adamantyl)-1 α ,25-dihydroxy-2-methylidene-23,23,24,24-tetrahydro-19,26,27-trinorvitamin D₃ 1,3-Bis(tert-butylidimethylsilyl) Ether 25-[(R)- α -Methoxy- α -(trifluoromethyl)]-phenylacetate (10a). To a solution of 25-hydroxyl compound **8a** (2.3 mg, 3.1 μmol) in CH_2Cl_2 (400 μL) were added Et_3N (4.3 μL , 0.031 mmol, 10 equiv) and DMAP (2.1 mg, 0.017 mmol, 5.6 equiv). To this solution was added at 0 °C a solution of (S)-(+)- α -methoxy- α -(trifluoromethyl)]-phenylacetyl chloride (MTPA-Cl, 3.8 mg, 0.016 mmol, 5 equiv) in CH_2Cl_2 (250 μL) and stirred at the same temperature for 10 min and then at room temperature for 45 min. DMAP (2.8 mg, 0.023 mmol, 7.5 equiv) was added to the mixture and stirred further at room temperature for 2 h. Ice water was added to the reaction, and the mixture was extracted with ethyl acetate, and the extracts were washed with saline, dried over MgSO_4 , and evaporated. The residue was chromatographed on silica gel to give **10a** (200 μg , 6.6%). **10a**: $^1\text{H NMR}$ (CDCl_3) δ 0.02, 0.05, 0.07, 0.08 (each 3 H, s, SiMe), 0.56 (3 H, s, 18-Me), 0.86, 0.90 (each 9 H, s, SiBu⁺), 1.10 (3 H, d, J = 6.4 Hz, 21-Me), 3.59 (3 H, s, OMe), 4.41–4.45 (2 H, m, H-1 and -3), 4.92, 4.97 (each 1 H, s, C=CH₂), 5.10 (1 H, s, H-25), 5.83 (1 H, d, J = 11.2 Hz, H-7), 6.21 (1 H, d, J = 11.2 Hz, H-6), 7.36–7.59 (5 H, m, phenyl).

(25R)-25-(1-Adamantyl)-1 α ,25-dihydroxy-2-methylidene-23,23,24,24-tetrahydro-19,26,27-trinorvitamin D₃ 1,3-Bis(tert-butylidimethylsilyl) Ether 25-[(S)- α -Methoxy- α -(trifluoromethyl)]-phenylacetate (10b). 25-Hydroxyl compound **8a** (3.0 mg, 4 μmol) was treated with (R)-(-)-MTPA-Cl to give (S)-MTPA ester (**10b**) (500 mg, 13%) similarly as above. **10b**: $^1\text{H NMR}$ (CDCl_3) δ 0.02, 0.05, 0.07, 0.08 (each 3H, s, SiMe), 0.56 (3 H, s, 18-Me), 0.86, 0.90 (each 9 H, s, SiBu⁺), 1.05 (3 H, d, J = 6.4 Hz, 21-Me), 3.55 (3 H, s, OMe), 4.41–4.45 (2 H, m, H-1 and -3), 4.92, 4.97 (each 1 H, s, C=CH₂), 5.06 (1 H, s, H-25), 5.83 (1 H, d, J = 11.2 Hz, H-7), 6.21 (1 H, d, J = 11.2 Hz, H-6), 7.36–7.59 (5H, m, phenyl).

26-(1-Adamantyl)-1 α ,25-dihydroxy-2-methylidene-23,23,24,24-tetrahydro-19,27-dinorvitamin D₃ 1,3-Bis(tert-butylidimethylsilyl) Ether 25-[(R)- α -Methoxy- α -(trifluoromethyl)]-phenylacetate (11a and 11b). 26-Adamantyl-25-hydroxyl compound **9** (5.2 mg, 6.8 μmol) was allowed to react with (S)-(+)-MTPA-Cl (8.9 mg, 38 μmol , 5.6 equiv) in the presence of Et_3N (9.5 μL , 68 μmol , 10 equiv) and DMAP (5 mg, 38 μmol , 5.6 equiv) similarly to

the above experiments. After work-up and chromatography on silica gel (5 g) with 2% ethyl acetate/hexane, (R)-MTPA ester **11** (5.4 mg, 81%) was obtained as a 1:1 mixture of epimers at C-25. The mixture was separated by HPLC [Hiber RT LiChrosorb Si 60 (7 μm), 250 mm \times 10 mm, CH_2Cl_2 /hexane 2/3 4.0 mL/min] to give less polar **11a** and more polar **11b**. **11a** (less polar): $^1\text{H NMR}$ (CDCl_3) δ 0.025, 0.05, 0.065, 0.08 (each 3 H, s, SiMe), 0.54 (3 H, s, 18-Me), 0.86, 0.90 (each 9 H, s, SiBu⁺), 1.04 (3 H, d, J = 6.4 Hz, 21-Me), 1.56–1.71 (2 H, overlapping, H-26), 3.53 (3 H, s, OMe), 4.41–4.45 (2H, m, H-1 and -3), 4.92, 4.97 (each 1 H, s, C=CH₂), 5.60 (1 H, t, J = 6.4 Hz, H-25), 5.83 (1 H, d, J = 11.2 Hz, H-7), 6.21 (1 H, d, J = 11.2 Hz, H-6), 7.37–7.56 (5 H, m, phenyl). **11b** (more polar): $^1\text{H NMR}$ (CDCl_3) δ 0.025, 0.05, 0.065, 0.08 (each 3H, s, SiMe), 0.54 (3 H, s, 18-Me), 0.86, 0.90 (each 9 H, s, SiBu⁺), 1.03 (3 H, d, J = 6.4 Hz, 21-Me), 1.45–1.88 (2 H, overlapping, H-26), 3.53 (3 H, s, OMe), 4.41–4.45 (2 H, m, H-1 and -3), 4.92, 4.97 (each 1 H, s, C=CH₂), 5.60 (1 H, t, J = 6.4 Hz, H-25), 5.83 (1 H, d, J = 11.2 Hz, H-7), 6.21 (1 H, d, J = 11.2 Hz, H-6), 7.37–7.56 (5 H, m, phenyl).

26-(1-Adamantyl)-1 α ,25-dihydroxy-2-methylidene-23,23,24,24-tetrahydro-19,27-dinorvitamin D₃ 1,3-Bis(tert-butylidimethylsilyl) Ether 25-[(S)- α -Methoxy- α -(trifluoromethyl)]-phenylacetate (11c and 11d). 26-Adamantyl-25-hydroxyl compound **9** (5.6 mg, 7.4 μmol) was allowed to react with (R)-(-)-MTPA-Cl (9.6 mg, 41 μmol , 5.6 equiv) in the presence of Et_3N (10 μL , 74 μmol , 10 equiv) and DMAP (5 mg, 41 μmol , 5.6 equiv) similarly to the above experiments. After work-up and chromatography on silica gel (5 g) with 2% ethyl acetate/hexane, (S)-MTPA ester **11** (3 mg, 41%) was obtained as a 1:1 mixture of epimers at C-25. The mixture was separated by HPLC [Hiber RT LiChrosorb Si 60 (7 μm), 250 mm \times 10 mm, CH_2Cl_2 /hexane 2/3 4.0 mL/min] to give less polar **11c** and more polar **11d**. **11c** (less polar): $^1\text{H NMR}$ (CDCl_3) δ 0.025, 0.05, 0.065, 0.08 (each 3 H, s, SiMe), 0.54 (3 H, s, 18-Me), 0.86, 0.90 (each 9 H, s, SiBu⁺), 1.04 (3 H, d, J = 6.4 Hz, 21-Me), 3.53 (3 H, s, OMe), 4.41–4.45 (2 H, m, H-1,3), 4.92, 4.97 (each 1 H, s, C=CH₂), 5.60 (1H, t, J = 6.4 Hz, H-25), 5.83 (1H, d, J = 11.2 Hz, H-7), 6.21 (1H, d, J = 11.2 Hz, H-6), 7.36–7.59 (5 H, m, phenyl). **11d** (more polar): $^1\text{H NMR}$ (CDCl_3) δ 0.025, 0.05, 0.065, 0.08 (each 3 H, s), 0.54 (3 H, s), 0.86, 0.90 (each 9 H, s), 1.03 (3 H, d, J = 6.4 Hz, 21-Me), 3.53 (3 H, s, OMe), 4.41–4.45 (2 H, m, H-1, 3), 4.92, 4.97 (each 1 H, s, C=CH₂), 5.60 (1 H, t, J = 6.4 Hz, H-25), 5.83 (1 H, d, J = 11.2 Hz, H-7), 6.21 (1H, d, J = 11.2 Hz, H-6), 7.38–7.56 (5 H, m, phenyl).

(25R)-25-(1-Adamantyl)-1 α ,25-dihydroxy-2-methylidene-23,23,24,24-tetrahydro-19,26,27-trinorvitamin D₃ (4a). The less polar **8a** (1.35 mg, 1.8 μmol) was treated with CSA (1.68 mg, 7.2 μmol , 4 equiv) in MeOH (500 μL) at room temperature for 3 h. Saturated NaHCO_3 solution was added to the reaction at 0 °C, the mixture was extracted with ethyl acetate, the extract was washed with saline, dried over MgSO_4 , and evaporated. The residue was chromatographed on Sephadex LH-20 (1 g) and eluted with CHCl_3 /hexane/MeOH 70/30/1 to give **4a** (880 μg , 94%). **4a** (ADTK2): $^1\text{H NMR}$ (CDCl_3) δ 0.57 (3 H, s, 18-Me), 1.10 (3 H, d, J = 6.4 Hz, 21-Me), 3.86 (1 H, s, H-25), 4.44–4.51 (2H, m, H-1, 3), 5.10, 5.11 (each 1H, s, C=CH₂), 5.89 (1H, d, J = 12 Hz, H-7), 6.36 (1H, d, J = 12 Hz, H-6). $^{13}\text{C NMR}$ (CDCl_3) δ 12.23, 19.41, 22.25, 23.45, 25.99, 27.47, 28.29, 28.94, 29.70, 35.73, 37.15, 37.50, 37.79, 38.15, 40.29, 45.70, 45.79, 55.32, 56.32, 70.71, 71.81, 71.93, 77.22, 80.26, 85.13, 107.77, 115.43, 124.20, 130.58, 143.13, 151.93. MS m/z (%): 518 (M^+ , 10), 365 (10), 347 (10), 295 (10), 135 (100), 93 (25), 79 (25). HRMS (DART) m/z calcd for $\text{C}_{35}\text{H}_{50}\text{O}_3$ (M^+) 518.376, found 518.368.

(25S)-25-(1-Adamantyl)-1 α ,25-dihydroxy-2-methylidene-23,23,24,24-tetrahydro-19,26,27-trinorvitamin D₃ (4b). The more polar **8b** (1.07 mg, 1.4 μmol) was similarly treated with CSA (1.31 mg, 5.6 μmol , 4 equiv) in MeOH (700 μL) at room temperature for 3 h. After similar work-up, the residue was chromatographed on Sephadex LH-20 (1 g) and eluted with CHCl_3 /hexane/MeOH 70/30/1 to give **4b** (683 μg , 91%). **4b** (ADTK1): $^1\text{H NMR}$ (CDCl_3) δ : 0.57 (3H, s, 18-Me), 1.10 (3H, d, J = 6.4 Hz, 21-Me), 3.86 (1H, d, J = 4 Hz, H-25), 4.46–4.50 (2H, m, H-1, 3), 5.10, 5.11 (each 1H, s, C=CH₂), 5.89 (1H, d, J = 12 Hz, H-7), 6.36 (1H, d, J = 12 Hz, H-6). $^{13}\text{C NMR}$ (CDCl_3) δ 12.23, 19.41, 22.25, 23.45, 25.98, 27.46, 28.30, 28.94, 29.70, 35.71, 37.15, 37.49, 37.80, 38.15, 40.29, 45.70, 45.79, 55.32, 56.32, 70.71, 71.81, 71.92, 77.21,

80.26, 85.13, 107.77, 115.43, 124.20, 130.58, 143.13, 151.94. MS m/z (%): 518 (M^+ , 10), 365 (10), 347 (10), 295 (10), 135 (100), 93 (25), 79 (25). HRMS (DART) m/z calcd for $C_{35}H_{50}O_3$ (M^+) 518.376, found 518.366.

(25R)-26-(1-Adamantyl)-1 α ,25-dihydroxy-2-methylidene-23,23,24,24-tetradehydro-19,27-dinorvitamin D₃ (5a). To a solution of the less polar isomer of *R*-MTPA ester **11a** (1.03 mg, 1 μ mol) in MeOH (500 μ L) was added a solution of CSA (1.22 mg, 5.2 μ mol, 5 equiv) in MeOH (200 μ L) at 0 °C, and the mixture was stirred at room temperature for 3 h. Saturated NaHCO₃ solution was added at 0 °C, the mixture was extracted with ethyl acetate, and the extract was washed with saline, dried over MgSO₄, and evaporated. The residue was dissolved in MeOH (600 μ L), K₂CO₃ (130 mg) was added, and the mixture was stirred at room temperature for 24 h. Saturated NH₄Cl solution was added to the reaction mixture at 0 °C, and the mixture was extracted with ethyl acetate. The extract was washed with saline, dried, and evaporated. The residue was chromatographed on Sephadex LH-20 (1 g) and eluted with CHCl₃/hexane/MeOH 70/30/1 to give **5a** (314 μ g, 56%). **5a** (ADTK3): ¹H NMR (CDCl₃) δ 0.56 (3 H, s, 18-Me), 1.07 (3 H, d, J = 6.4 Hz, 21-Me), 4.45–4.53 (3 H, m, H-1, -3, and 25), 5.10, 5.11 (each 1 H, s, C=CH₂), 5.88 (1H, d, J = 11.2 Hz, H-7), 6.36 (1H, d, J = 11.2 Hz, H-6). MS m/z (%): 532 (M^+ , 10), 429 (10), 361 (10), 309 (10), 135 (100), 93 (40), 79 (40). HRMS (DART) m/z calcd for $C_{36}H_{52}O_3$ (M^+) 532.392, found 532.373.

The more polar isomer of *S*-MTPA ester **11d** was similarly hydrolyzed to give **5a**.

(25S)-26-(1-Adamantyl)-1 α ,25-dihydroxy-2-methylidene-23,23,24,24-tetradehydro-19,27-dinorvitamin D₃ (5b). The more polar isomer of longer side chain (*R*)-Mosher ester **11b** (1.05 mg, 1.1 mmol) was deprotected similarly to the above experiment. After purification by Sephadex LH-20 (1 g) column chromatography, **5b** (383 μ g, 67%) was obtained. **5b** (ADTK4): ¹H NMR (CDCl₃) δ 0.56 (3 H, s, 18-Me), 1.07 (3 H, d, J = 6.4 Hz, 21-Me), 4.45–4.53 (3 H, m, H-1, -3, and -25), 5.10, 5.11 (each 1 H, s, C=CH₂), 5.88 (1H, d, J = 11.2 Hz, H-7), 6.36 (1H, d, J = 11.2 Hz, H-6). MS m/z (%): 532 (M^+ , 10), 429 (10), 361 (10), 309 (10), 135 (100), 93 (40), 79 (40). HRMS (DART) m/z calcd for $C_{36}H_{52}O_3$ (M^+) 532.392, found 532.368.

The less polar isomer of *S*-MTPA ester **11c** was similarly hydrolyzed to give **5b**.

25-(1-Adamantyl)-1 α -hydroxy-2-methylidene-25-oxo-23,23,24,24-tetradehydro-19,26,27-trinorvitamin D₃ 1,3-Bis-(tert-butylidimethylsilyl) Ether (12a). To a solution of an epimeric mixture at C(25) of **8** (39.0 mg, 52 μ mol) in CH₂Cl₂ (1.4 mL) was added Dess–Martin periodinane (DMP, 85.9 mg, 202 μ mol, 4 equiv) and stirred at room temperature for 4 h. Saturated Na₂SO₃ solution was added to the reaction, and the mixture was extracted with CH₂Cl₂, and the extracts were washed with saline, dried over MgSO₄, and evaporated. The residue was chromatographed on silica gel to give **12a** (32.8 mg, 84%). **12a**: ¹H NMR (CDCl₃) δ 0.03, 0.05, 0.07, 0.08 (each 3 H, s, SiMe), 0.57 (3 H, s, 18-Me), 0.86, 0.90 (each 9 H, s, SiBu^t), 1.14 (3 H, d, J = 6.8 Hz, 21-Me), 4.40–4.45 (2 H, m, H-1 and -3), 4.93, 4.97 (each 1 H, s, C=CH₂), 5.85 (1 H, d, J = 11.2 Hz, H-7), 6.21 (1 H, d, J = 11.2 Hz, H-6). ¹³C NMR (CDCl₃) δ -4.90, -4.85, 0.22, 12.17, 18.16, 18.24, 19.55, 22.17, 23.33, 25.78, 25.84, 26.40, 27.69, 27.91, 28.67, 35.60, 36.56, 38.12, 38.59, 40.42, 45.63, 46.73, 47.62, 55.49, 56.23, 71.63, 72.51, 77.20, 80.12, 94.57, 106.31, 116.40, 122.28, 133.11, 140.59, 152.93, 194.06. MS m/z (%): 745 (M^+ , 1), 612 (36), 383 (10), 366 (20), 229 (100), 135 (30), 73 (50). HRMS (DART) m/z calcd for $C_{47}H_{77}O_4Si_2$ (M^+ + OH) 761.536, found 761.528.

26-(1-Adamantyl)-1 α -hydroxy-2-methylidene-25-oxo-23,23,24,24-tetradehydro-19,27-dinorvitamin D₃ 1,3-Bis-(tert-butylidimethylsilyl) Ether (12b). To a solution of **9** (29.7 mg, 39 μ mol) in CH₂Cl₂ (1.4 mL) was added DMP (46.7b mg, 110 μ mol, 2.8 equiv), and the mixture was stirred at room temperature for 2.5 h. Saturated Na₂SO₃ solution was added to the reaction, and the mixture was extracted with CH₂Cl₂, and the extracts were washed with saline, dried over MgSO₄, and evaporated. The residue was chromatographed on silica gel to give **12b** (20.1 mg, 68%). **12b**: ¹H NMR (CDCl₃) δ 0.03, 0.05, 0.06, 0.08 (each 3 H, s, SiMe), 0.56 (3 H, s, 18-Me), 0.86, 0.90 (each 9 H, s, SiBu^t), 1.12 (3 H, d, J = 6.8 Hz, 21-Me), 2.15 (2 H, s, H-26),

4.40–4.46 (2 H, m, H-1 and -3), 4.92, 4.98 (each 1 H, s, C=CH₂), 5.84 (1 H, d, J = 11.2 Hz, H-7), 6.21 (1 H, d, J = 11.2 Hz, H-6). MS m/z (%): 759 (M^+ , 2), 701 (3), 626 (40), 383 (10), 366 (30), 243 (30), 135 (100), 73 (50). HRMS (DART) m/z calcd for $C_{48}H_{79}O_4Si_2$ (M^+ + OH) 775.552, found 775.588.

Stereo Selective Reduction of 12a with (4R)-2-Methyl-4,5,5-triphenyl-1,3,2-oxazaborolidine. To a solution of 25-keto compound **12a** (6.1 mg, 8.2 μ mol) in THF (10 μ L) was added a solution of (*R*)-BMTO (4.0 mg, 13 μ mol, 1.6 equiv) and borane–dimethyl sulfide complex (BMS, 10.0–10.2 M, 1.4 μ L, 14 μ mol, 1.7 equiv) in THF (25 μ L) at 0 °C, and the mixture was stirred for 1 h. MeOH was added at 0 °C, and the mixture was evaporated. The residue was chromatographed on silica gel (4.7 g) and eluted with 5% ethyl acetate/hexane to give **8a** (4.3 mg, 5.8 μ mol 70%, 78% de). **8a**: ¹H NMR (CDCl₃) δ 0.02, 0.05, 0.06, 0.08 (each 3 H, s, SiMe), 0.56 (3 H, s, 18-Me), 0.86, 0.90 (each 9 H, s, SiBu^t), 1.11 (3 H, d, J = 6.4 Hz, 21-Me), 3.86 (1 H, s, H-25), 4.41–4.45 (2 H, m, H-1 and -3), 4.92, 4.97 (each 1 H, s, C=CH₂), 5.84 (1 H, d, J = 11.2 Hz, H-7), 6.21 (1 H, d, J = 11.2 Hz, H-6). MS m/z (%): 746 (M^+ , 2), 614 (18), 596 (20), 366 (20), 234 (12), 135 (100), 73 (80).

Stereo Selective Reduction of 12a with (R)-3,3-Diphenyl-1-methyltetrahydro-1H,3H-pyrrolo[1,2-c][1,3,2]oxazaborole. To a solution of 25-keto compound **12a** (4.4 mg, 5.9 μ mol) in THF (20 μ L) was added a solution of (*R*)-CBS (2.1 mg, 7.6 μ mol, 1.3 equiv) and BMS (10.0–10.2 M, 0.8 μ L, 8.0 μ mol, 1.3 equiv) in THF (14 μ L) at 0 °C, and the mixture was stirred for 50 min. MeOH was added at 0 °C, and the mixture was evaporated. The residue was chromatographed on silica gel (5.5 g) and eluted with 5% ethyl acetate/hexane to give **8a** (3.8 mg, 86%, and 91% de).

Stereo Selective Reduction of 12a with (S)-3,3-Diphenyl-1-methyltetrahydro-1H,3H-pyrrolo[1,2-c][1,3,2]oxazaborole. To a solution of 25-keto compound **12a** (23.6 mg, 32 μ mol) in THF (100 μ L) was added a solution of (*S*)-CBS (12.5 mg, 45 μ mol, 1.4 equiv) and BMS (10.0–10.2 M, 4.5 μ L, 45 μ mol, 1.4 equiv) in THF (80 μ L) at 0 °C, and the mixture was stirred for 50 min. After similar work-up, the residue was chromatographed on silica gel to give **8b** (17.8 mg, 75%, 87% de) and recovered **12a** (2.2 mg, 9.3%). **8b**: ¹H NMR (CDCl₃) δ 0.02, 0.05, 0.07, 0.08 (each 3 H, s, SiMe), 0.56 (3 H, s, 18-Me), 0.86, 0.90 (each 9 H, s, SiBu^t), 1.10 (3 H, d, J = 2.4 Hz, 21-Me), 3.86 (1 H, s, H-25), 4.41–4.45 (2 H, m, H-1 and -3), 4.92, 4.97 (each 1 H, s, C=CH₂), 5.84 (1 H, d, J = 11.2 Hz, H-7), 6.21 (1 H, d, J = 11.2 Hz, H-6). MS m/z (%): 746 (M^+ , 2), 614 (18), 596 (20), 366 (20), 234 (12), 135 (100), 73 (80).

Stereo Selective Reduction of 12b with a (R)-3,3-Diphenyl-1-methyltetrahydro-1H,3H-pyrrolo-[1,2-c][1,3,2]oxazaborole. Similarly, one-carbon longer homologue **9a** (**25R**) was synthesized from **12b** (2.1 mg, 2.7 μ mol) by reduction with (*R*)-CBS (2.2 mg, 7.9 μ mol, 2.9 equiv) and BMS (10.0–10.2 M, 0.92 μ L, 9.2 μ mol, 3.4 equiv) in THF (180 μ L). After chromatography on silica gel (6.0 g) with 5% ethyl acetate/hexane, **9a** (1.4 mg, 1.9 μ mol, 68%, >95%de) was obtained. **9a**: ¹H NMR (CDCl₃) δ 0.02, 0.05, 0.06, 0.08 (each 3 H, s, SiMe), 0.55 (3 H, s, 18-Me), 0.86, 0.90 (each 9 H, s, SiBu^t), 1.06 (3 H, d, J = 8.0 Hz, 21-Me), 4.41–4.45 (2 H, m, H-1 and -3), 4.51 (1 H, m, 25-H), 4.92, 4.97 (each 1 H, s, C=CH₂), 5.84 (1 H, d, J = 11.2 Hz, H-7), 6.21 (1 H, d, J = 11.2 Hz, H-6). MS m/z (%): 760 (M^+ , 2), 610 (16), 475 (18), 366 (20), 234 (12), 135 (100), 73 (75).

Stereo Selective Reduction of 12b with a (S)-3,3-Diphenyl-1-methyltetrahydro-1H,3H-pyrrolo[1,2-c][1,3,2]oxazaborole. Similarly, one-carbon longer homologue **9b** (**25S**) was synthesized from **12b** (2.1 mg, 2.7 μ mol) by reduction with (*S*)-CBS (2.2 mg, 7.8 μ mol, 2.8 equiv) and BMS (10.0–10.2 M, 0.92 μ L, 9.2 μ mol, 3.4 equiv) in THF (180 μ L). After chromatography on silica gel (6.0 g) with 5% ethyl acetate/hexane, **9b** (1.3 mg, 1.7 μ mol, 62%, >95% de) was obtained. **9b**: ¹H NMR (CDCl₃) δ 0.02, 0.05, 0.06, 0.08 (each 3 H, s, SiMe), 0.55 (3 H, s, 18-Me), 0.86, 0.90 (each 9 H, s, SiBu^t), 1.06 (3 H, d, J = 8.0 Hz, 21-Me), 4.41–4.45 (2 H, m, H-1 and -3), 4.51 (1 H, m, 25-H), 4.92, 4.97 (each 1 H, s, C=CH₂), 5.84 (1 H, d, J = 11.2 Hz, H-7), 6.21 (1 H, d, J = 11.2 Hz, H-6). MS m/z (%): 760 (M^+ , 2), 610 (16), 475 (18), 366 (20), 234 (12), 135 (100), 73 (75).

Cell Lines and Cell Cultures. Human kidney HEK293 cells (RIKEN Cell Bank, Tsukuba, Japan) were cultured in Dulbecco's Modified Eagle's Medium (DMEM) containing 5% inactivated fetal

bovine serum (FBS), 100 U/mL penicillin, and 0.1 mg/mL streptomycin (Nacalai Tesque, Kyoto, Japan). Human colon carcinoma SW480 cells (American Type Culture Collection, Manassas, VA) and immortalized keratinocyte HaCaT cells (kindly provided by Dr. Tadashi Terui, Department of Dermatology, Nihon University School of Medicine) were cultured in DMEM containing 10% FBS, 100 U/mL penicillin, and 0.1 mg/mL streptomycin. Human osteosarcoma MG63 cells (RIKEN Cell Bank) were cultured in minimum essential medium containing 10% FBS, 100 U/mL penicillin, and 0.1 mg/mL streptomycin. Human myeloid leukemia THP-1 cells and U937 cells (RIKEN Cell Bank) were cultured in RPMI1640 medium containing 10% FBS, 100 U/mL penicillin, and 0.1 mg/mL streptomycin. The condition of cell culturing was kept at 37 °C in a humidified atmosphere containing 5% CO₂.

Plasmids. The expression vectors pCMX-VDR, pCMX-RXR α , pCMX-VP16-VDR, pCMX-GAL4-RXR α , pCMX-GAL4-SRC-1, pCMX-GAL4-N-CoR, and pCMX-GAL4-SMART were reported previously.^{13b} The nuclear receptor-interacting domains of SRC-1 (amino acids 595–771; GenBank accession no. U90661), N-CoR (amino acids 1990–2416; GenBank accession no. U35312), and SMRT (amino acids 2003–2517; GenBank accession no. AF113003) were inserted into the pCMX-GAL4 vector to make pCMX-GAL4-SRC-1, pCMX-GAL4-N-CoR, and pCMX-GAL4-SMRT, respectively. VDR responsive Spp \times 3-tk-LUC and GAL4-responsive MH100(UAS) \times 4-tk-LUC reporter vectors were previously reported.^{14d} pGEX vector (GE Healthcare, Chalfont St. Giles, Buckinghamshire, UK) was used to generate glutathione transferase (GST) fusions.³⁰ The human recombinant VDR ligand-binding domain (LBD) (amino acids 140–427) was inserted into pGEX vector to generate pGEX-VDR.

Vitamin D Receptor-Binding Assay. The pGEX or pGEX-hVDR was expressed as a GST fusion protein in *Escherichia coli* BL21 (EMD Millipore). The cells were lysed by sonication in sonication buffer (50 mM Tris-HCl pH 8.0, 50 mM NaCl, 1 mM EDTA, and 1 mM DTT). Then 1 μ g of the supernatants was diluted in binding buffer (25 mM Tris pH 7.5, 100 mM KCl, 25 mM DTT, 4 mM CHAPS, pH 7.5) containing bovine serum albumin (100 μ g/mL). A solution containing an increasing amount of 1,25(OH)₂D₃ (1) or synthetic analogues in 15 μ L of EtOH was added to 570 μ L of the receptor solution in each tube, and the mixture was vortexed 2–3 times. The mixture was incubated for 30 min at room temperature. [26,27-Methyl-³H] 1,25(OH)₂D₃ (PerkinElmer) in 15 μ L of EtOH was added, vortexed 2–3 times, and the whole mixture was then allowed to stand at 4 °C for 20 h. At the end of the second incubation, 400 μ L of dextran-coated charcoal solution (Sigma) was added to bind any free ligands (or to remove free ligands) and the sample was vortexed. After 30 min at room temperature, bound and free [³H]-1,25(OH)₂D₃ were separated by centrifugation at 3000 rpm for 10 min at 0 °C. Aliquots (800 μ L) of the supernatant were mixed with 9.2 mL of Bio Fluor (PerkinElmer) and submitted for radioactivity counting. Each assay was performed at least twice in triplicate.

Transcription Assays. HEK293 cells were cultured in Dulbecco's Modified Eagle's Medium containing 5% fetal bovine serum and antibiotic-antimycotics (Nacalai) at 37 °C in a humidified atmosphere of 5% CO₂ in air. Transfections of 50 ng of TK-Spp \times 3-LUC reporter plasmid, 10 ng of pCMX- β -galactosidase, 15 ng of pCMX-VDR, and 15 ng of pCMX-RXR α for each well of a 96-well plate were performed by the calcium phosphate coprecipitation method as described previously.^{14d} Then 18 h after transfection, test compounds were added. Cells were harvested after 16–24 h for luciferase and β -galactosidase activity using a luminometer (Molecular Devices, Sunnyvale, CA).

Mammalian two-hybrid assay for cofactor interaction to VDR was used 50 ng of TK-MH100(UAS) \times 4-LUC reporter plasmid, 10 ng of pCMX- β -galactosidase, 15 ng of pCMX-GAL4-RXR α , pCMX-GAL4-SRC1, pCMX-GAL4-N-CoR, or pCMX-GAL4-SMRT and 15 ng of pCMX-VP16-VDR for each well of a 96-well plate. Luciferase data were normalized to the internal β -galactosidase control.

Reverse Transcription and Quantitative Real-Time PCR Analysis. For gene expression analysis, 1 \times 10⁴ cells per well were plated in 24 well plate. After 24 h, cells were treated with ethanol control or 100 nM of 1,25(OH)₂D₃ or its analogues for 24 h. Total RNAs from samples were prepared by the acid guanidine thiocyanate-phenol/

chloroform method.³¹ cDNAs were synthesized using the ImProm-II reverse transcription system (Promega, Madison, WI).^{14d} Real-time PCR was performed on the ABI PRISM 7000 sequence detection system (Applied Biosystems, Foster City, CA) using Power SYBR Green PCR Master Mix (Applied Biosystems). Primer sequences were as follows: CYP24A1:5'-TGAACGTTGGCTTCAGGAGAA-3' and 5'-AGGGTGCCTGAGTGTAGCATCT-3', TRPV6:5'-TGAACGTTGGCTTCAGGAGAA-3' and 5'-AGGGTGCCTGAGTGTAGCATCT-3', CAMP 5'-GCTAACCTC-TACCGCCTCCT-3' and 5'-GGTCACTGTCCCCATACACC-3', and ACTIN: 5'-GACAGGATGCAGAAGGAGAT-3' and 5'-GAAG-CATTTGCGGTGGACGAT-3'. mRNA values were normalized to an amount of ACTIN mRNA.

Protein Expression and Purification. The rat VDR LBD (residues 116–423, Δ 165–211) was cloned as an N-terminal His6-tagged fusion protein into the pET14b expression vector and was overexpressed in *E. coli* C41. The cells were grown at 37 °C in LB medium (including 100 mg/L ampicillin) and were subsequently induced for 6 h with 15 μ M isopropyl- β -D-thiogalactopyranoside (IPTG) at 23 °C. The purification procedure included affinity chromatography on a Ni-NTA column, followed by dialysis and ion-exchange chromatography (SP-Sepharose). After tag removal by thrombin digestion, the protease was removed by filtration through a HiTrap benzamide column, and the protein was further purified by gel filtration on a Superdex 200 column. The purity and homogeneity of the rVDR LBP were assessed by SDS-PAGE.

Crystallization. Purified rVDR-LBD solution was concentrated to about 0.75 mg/mL by ultrafiltration. To an aliquot (800 μ L) of the protein solution was added a ligand (4a, 4b, 5a or 5b, ca. 10 equiv); the solution was further concentrated to about 1/8, and then a solution (25 mM Tris-HCl, pH 8.0; 50 mM NaCl; 10 mM DTT; 0.02% Na₃N) of coactivator peptide (H2N-KNHPMLMNLKDN-CONH₂) derived from DRIP205 was added. This solution of VDR/ligand/peptide was allowed to crystallize by the vapor-diffusion method that used a series of precipitant solutions containing 0.1 M MOPS-NaOH (pH 7.0), 0.1–0.4 M sodium formate, 12–22% (w/v) PEG4000, and 5% (v/v) ethylene glycol. Droplets for crystallization were prepared by mixing 2 μ L of complex solution and 1 μ L of precipitant solution, and droplets were equilibrated against 500 μ L of precipitant solution at 20 °C. It took 1–2 days to obtain crystals of X-ray diffraction quality for VDR complexes with 4a, 4b, 5a, or 5b as a ligand.

Diffraction Experiment and Structure Analysis. Prior to the diffraction data collection, crystals were soaked in a cryoprotectant solution that contained 0.1 M MOPS-NaOH (pH 7.0), 0.1–0.4 M sodium formate, 15–20% PEG4000, and 17–20% ethylene glycol. Diffraction data sets were collected at 100 K in a stream of nitrogen gas at beamlines BL-6A of KEK-PF and NW12A of PF-AR (Tsukuba, Japan). Reflections were recorded with an oscillation range per image of 1.0°. Diffraction data were indexed, integrated, and scaled using the program HKL2000.³² The structures of the complex were solved by molecular replacement with the program CNS,³³ and finalized sets of atomic coordinates were obtained after iterative rounds of model modification with the program XtalView³⁴ and after refinement with CNS by rigid body refinement, simulated annealing, positional minimization, water molecule identification, and individual isotropic B-value refinement.

■ ASSOCIATED CONTENT

☛ Supporting Information

The X-ray crystal structure of rVDR-LBD complexed with ADTK2 (4a); unit cell structures of the ternary rVDR-LBD complexes with 4b (ADTK1), 5a (ADTK3 or 1,25(OH)₂D₃ (1), and DRIP205; inter unit-cell interactions in the rVDR-LBD complex with 4b; ternary rVDR-LBD complexes with ligands (4b, 5a, and 5b) and DRIP205 peptide in canonical active conformations; summary of data collection statistics and refinement; X-ray crystal data of compound 4a (ADTK2). This material is available free of charge via the Internet at <http://pubs.acs.org>.

Accession Codes

PDB codes for **4b**, **5a**, and **5b** are 3VTB, 3VTC and 3VTD, respectively.

AUTHOR INFORMATION

Corresponding Authors

*For S.Y.: Phone, +81 3 3972 8111 ext 2363; E-mail, yamada.vd@image.ocn.ne.jp.

*For M.M.: Phone, +81 3 3972 8111 ext 2243; E-mail, makishima.makoto@nihon-u.ac.jp.

Author Contributions

[†]These authors contributed equally.

Notes

The authors declare no competing financial interest.

ACKNOWLEDGMENTS

Part of this work was supported by an Adaptable and Seamless Technology Transfer Program Feasibility Study (AS232Z02361G) from Japan Science and Technology Agency. This work was also supported in part by Grants-in-Aid for Scientific Research (grant no. 25460394) from JSPS and Grants-in-Aid for Scientific Research (C) (grant no. 25460157) from MEXT. We acknowledge MEXT Supported Program for the Strategic Research Foundation at Private Universities, 2013–2018. The synchrotron-radiation experiment was performed at the Photon Factory. We acknowledge the help provided by the beamlines scientists at the Photon Factory. We thank professor Hector F. DeLuca at the Department of Biochemistry, University of Wisconsin—Madison, for providing an expression plasmid of the rVDR-LBD.

ABBREVIATIONS USED

DMP, dimethylaminopyridine; CSA, camphor sulfonic acid; DMP, Dess–Martin periodinane; CBS, Corey–Bakshi–Shibata; RXR α , retinoid X receptor α ; SRC-1, steroid receptor coactivator 1; NCoA1, nuclear receptor coactivator 1; N-CoR, nuclear receptor corepressor 1; SMRT, silencing mediator of retinoic acid and thyroid hormone receptor; N-CoR2, nuclear receptor corepressor 2; AF2, activation function 2; CAMP, cathelicidin antimicrobial peptides; TRPV6, transient receptor potential vanilloid 6; MTPA, α -methoxy- α -(trifluoromethyl)-phenyl-acetyl; BMTO, B-methyl-4,5,5-triphenyl-1,3,2-oxazaborolidine; BMS, borane–dimethyl sulfide complex

REFERENCES

- (1) Pike, J. W.; Zella, L. A.; Meyer, M. B.; Fretz, J. A.; Kim, S. Molecular actions of 1,25-dihydroxyvitamin D3 on genes involved in calcium homeostasis. *J. Bone Miner. Res.* **2007**, *22* (Suppl 2), V16–V19.
- (2) Lacey, D. L.; Timms, E.; Tan, H. L.; Kelley, M. J.; Dunstan, C. R.; Burgess, T.; Elliott, R.; Colombero, A.; Elliott, G.; Scully, S.; Hsu, H.; Sullivan, J.; Hawkins, N.; Davy, E.; Capparelli, C.; Eli, A.; Qian, Y. X.; Kaufman, S.; Sarosi, I.; Shalhoub, V.; Senaldi, G.; Guo, J.; Delaney, J.; Boyle, W. J. Osteoprotegerin ligand is a cytokine that regulates osteoclast differentiation and activation. *Cell* **1998**, *93*, 165–176.
- (3) Yasothan, U.; Kar, S. Osteoporosis: overview and pipeline. *Nature Rev. Drug Discovery* **2008**, *7*, 725–726.
- (4) Kawai, M.; Mödder, U. I.; Khosla, S.; Rosen, C. J. Emerging therapeutic opportunities for skeletal restoration. *Nature Rev. Drug Discovery* **2011**, *10*, 141–156.
- (5) Chitre, M.; Shechter, D.; Grauer, A. Denosumab for treatment of postmenopausal osteoporosis. *Am. J. Health-Syst. Pharm.* **2011**, *68*, 1409–1418.
- (6) Cummings, S. R.; San Martin, J.; McClung, M. R.; Siris, E. S.; Eastell, R.; Reid, I. R.; Delmas, P.; Zoog, H. B.; Austin, M.; Wang, A.;

Kutilek, S.; Adami, S.; Zanchetta, J.; Libanati, C.; Siddhanti, S.; Christiansen, C. Denosumab for prevention of fractures in postmenopausal women with osteoporosis. *N. Engl. J. Med.* **2009**, *361*, 756–765.

(7) Xue, Y.; Karaplis, A. C.; Hendy, G. N.; Goltzman, D.; Miao, D. Exogenous 1,25-dihydroxyvitamin D3 exerts a skeletal anabolic effect and improves mineral ion homeostasis in mice that are homozygous for both the α -hydroxylase and parathyroid hormone null alleles. *Endocrinology* **2006**, *147*, 4801–4810.

(8) Kubodera, N. D-Hormone derivatives for the treatment of osteoporosis: from alfacalcidol to eldcalcitol. *Mini-Rev. Med. Chem.* **2009**, *9*, 1416–1422.

(9) Shevde, N. K.; Plum, L. A.; Clagett-Dame, M.; Yamamoto, H.; Pike, J. W.; DeLuca, H. F. A potent analog of 1 α ,25-dihydroxyvitamin D3 selectively induces bone formation. *Proc. Natl. Acad. Sci. U. S. A.* **2002**, *99*, 13487–13491. Plum, L. A.; Fitzpatrick, L. A.; Ma, X.; Binkley, N. C.; Zella, J. B.; Clagett-Dame, M.; DeLuca, H. F. 2MD, a new anabolic agent for osteoporosis treatment. *Osteoporosis Int.* **2006**, *17*, 704–715.

(10) DeLuca, H. F.; Bedale, W.; Binkley, N.; Gallagher, J. C.; Bolognese, M.; Peacock, M.; Aloia, J.; Clagett-Dame, M.; Plum, L. The vitamin D analog 2MD increases bone turnover but not BMD in postmenopausal women with osteopenia: results of a 1-year phase 2 double-blind, placebo-controlled, randomized clinical trial. *J. Bone Miner. Res.* **2011**, *26*, 538–545.

(11) Ma, Y.; Khalifa, B.; Yee, Y. K.; Lu, J.; Memezawa, A.; Savkur, R. S.; Yamamoto, Y.; Chintalacharuvu, S. R.; Yamaoka, K.; Stayrook, K. R.; Bramlett, K. S.; Zeng, Q. Q.; Chandrasekhar, S.; Yu, X. P.; Linebarger, J. H.; Iturria, S. J.; Burris, T. P.; Kato, S.; Chin, W. W.; Nagpal, S. Identification and characterization of noncalcemic, tissue-selective, nonsecosteroidal vitamin D receptor modulators. *J. Clin. Invest.* **2006**, *116*, 892–904.

(12) Shiau, A. K.; Barstad, D.; Loria, P. M.; Cheng, L.; Kushner, P. J.; Agard, D. A.; Greene, G. L. The structural basis of estrogen receptor/coactivator recognition and the antagonism of this interaction by tamoxifen. *Cell* **1998**, *95*, 927–937.

(13) (a) Lusher, S. J.; Raaijmakers, H. C.; Vu-Pham, D.; Kazemier, B.; Bosch, R.; McGuire, R.; Azevedo, R.; Hamersma, H.; Dechering, K.; Oubrie, A.; van Duin, M.; de Vlieg, J. X-ray structures of progesterone receptor ligand binding domain in its agonist state reveal differing mechanisms for mixed profiles of 11 β -substituted steroids. *J. Biol. Chem.* **2012**, *287*, 20333–20343. (b) Lusher, S. J.; Raaijmakers, H. C.; Vu-Pham, D.; Dechering, K.; Lam, T. W.; Brown, A. R.; Hamilton, N. M.; Nimz, O.; Bosch, R.; McGuire, R.; Oubrie, A.; de Vlieg, J. Structural basis for agonism and antagonism for a set of chemically related progesterone receptor modulators. *J. Biol. Chem.* **2011**, *286*, 35079–35086.

(14) (a) Igarashi, M.; Yoshimoto, N.; Yamamoto, K.; Shimizu, M.; Ishizawa, M.; Makishima, M.; DeLuca, H. F.; Yamada, S. Identification of a highly potent vitamin D receptor antagonist: (25S)-26-adamantyl-25-hydroxy-2-methylene-22,23-didehydro-19,27-dinor-20-epi-vitamin D3 (ADMI3). *Arch. Biochem. Biophys.* **2007**, *460*, 240–253. (b) Inaba, Y.; Yamamoto, K.; Yoshimoto, N.; Matsunawa, M.; Uno, S.; Yamada, S.; Makishima, M. Vitamin D₃ derivatives with adamantane or lactone ring side chains are cell type-selective vitamin D receptor modulators. *Mol. Pharmacol.* **2007**, *71*, 1298–1311. (c) Nakabayashi, M.; Yamada, S.; Yoshimoto, N.; Tanaka, T.; Igarashi, M.; Ikura, T.; Ito, N.; Makishima, M.; Tokiwa, H.; DeLuca, H. F.; Shimizu, M. Crystal structures of rat vitamin D receptor bound to adamantyl vitamin D analogs: structural basis for vitamin D receptor antagonism and partial agonism. *J. Med. Chem.* **2008**, *51*, 5320–5329. (d) Inaba, Y.; Yamamoto, K.; Yoshimoto, N.; Matsunawa, M.; Uno, S.; Yamada, S.; Makishima, M. Vitamin D₃ derivatives with adamantane or lactone ring side chains are cell type-selective vitamin D receptor modulators. *Mol. Pharmacol.* **2007**, *71*, 1298–1311.

(15) (a) Itsuno, S.; Ito, K.; Hirao, A.; Nakahama, S. Asymmetric reduction of aromatic ketones with the reagent prepared from (S)-(-)-2-amino-3-methyl-1,1-diphenylbutan-1-ol and borane. *J. Chem. Soc.: Chem. Commun.* **1983**, *8*, 469. (b) Corey, E. J.; Bakshi, R. K.; Shibata, S. Highly enantioselective borane reduction of ketones catalyzed by chiral oxazaborolidines. Mechanism and synthetic

implications. *J. Am. Chem. Soc.* **1987**, *109*, 5551–5553. (c) Corey, E. J.; Helal, C. J. Reduction of Carbonyl Compounds with Chiral Oxazaborolidine Catalysts: A New Paradigm for Enantioselective Catalysis and a Powerful New Synthetic Method. *Angew. Chem., Int. Ed.* **1998**, *37*, 1986–2012. (d) Bach, J.; Berenguer, R.; Garcia, J.; Loscertales, T.; Vilarrasa, J. Highly Enantioenriched Propargylic Alcohols by Oxazaborolidine-Mediated Reduction of Acetylenic Ketones. *J. Org. Chem.* **1996**, *61*, 9021–9025.

(16) (a) Ohtani, I.; Kusumi, T.; Kashman, Y.; Kakisawa, H.; High-field, F. T. NMR application of Mosher's method. The absolute configurations of marine terpenoids. *J. Am. Chem. Soc.* **1991**, *113*, 4092–4096. (b) Kusumi, T.; Fujita, Y.; Ohtani, I.; Kakisawa, K. Anomaly in the modified Mosher's method: absolute configurations of some marine membranolides. *Tetrahedron Lett.* **1991**, *32*, 2923–2926.

(17) Kobayashi, E.; Shimazaki, M.; Miyamoto, Y.; Masuno, H.; Yamamoto, K.; DeLuca, H. F.; Yamada, S.; Shimizu, M. Structure–activity relationships of 19-norvitamin D analogs having a fluoroethylene group at the C-2 position. *Bioorg. Med. Chem.* **2007**, *15*, 1475–1482.

(18) Ishizawa, M.; Matsunawa, M.; Adachi, R.; Uno, S.; Ikeda, K.; Masuno, H.; Shimizu, M.; Iwasaki, K.; Yamada, S.; Makishima, M. Lithocholic acid derivatives act as selective vitamin D receptor modulators without inducing hypercalcemia. *J. Lipid Res.* **2008**, *49*, 763–772.

(19) MacDonald, P. N.; Dowd, D. R.; Nakajima, S.; Galligan, M. A.; Reeder, M. C.; Haussler, C. A.; Ozato, K.; Haussler, M. R. Retinoid X receptors stimulate and 9-*cis*-retinoic acid inhibits 1,25-dihydroxyvitamin D₃-activated expression of the rat osteocalcin gene. *Mol. Cell. Biol.* **1993**, *13*, 5907–5917.

(20) Choi, M.; Yamada, S.; Makishima, M. Dynamic and ligand-selective interactions of vitamin D receptor with retinoid X receptor and cofactors in living cells. *Mol. Pharmacol.* **2011**, *80*, 1147–1155.

(21) Onate, S. A.; Boonyaratanakornkit, V.; Spencer, T. E.; Tsai, S. Y.; Tsai, M. J.; Edwards, D. P.; O'Malley, B. W. The steroid receptor coactivator-1 contains multiple receptor interacting and activation domains that cooperatively enhance the activation function 1 (AF1) and AF2 domains of steroid receptors. *J. Biol. Chem.* **1998**, *273*, 12101–12108.

(22) Underhill, C.; Qutob, M. S.; Yee, S. P.; Torchia, J. A novel nuclear receptor corepressor complex, N-CoR, contains components of the mammalian SWI/SNF complex and the corepressor KAP-1. *J. Biol. Chem.* **2000**, *275*, 40463–40470.

(23) Park, E. J.; Schroen, D. J.; Yang, M.; Li, H.; Li, L.; Chen, J. D. SMRTe, a silencing mediator for retinoid and thyroid hormone receptors-extended isoform that is more related to the nuclear receptor corepressor. *Proc. Natl. Acad. Sci. U. S. A.* **1999**, *96*, 3519–3524.

(24) Chen, K. S.; Prahl, J. M.; DeLuca, H. F. Isolation and expression of human 1,25-dihydroxyvitamin D₃ 24-hydroxylase cDNA. *Proc. Natl. Acad. Sci. U. S. A.* **1993**, *90*, 4543–4547.

(25) Liu, P. T.; Stenger, S.; Li, H.; Wenzel, L.; Tan, B. H.; Krutzik, S. R.; Ochoa, M. T.; Schaubert, J.; Wu, K.; Meinken, C.; Kamen, D. L.; Wagner, M.; Bals, R.; Steinmeyer, A.; Zügel, U.; Gallo, R. L.; Eisenberg, D.; Hewison, M.; Hollis, B. W.; Adams, J. S.; Bloom, B. R.; Modlin, R. L. Toll-like receptor triggering of a vitamin D-mediated human antimicrobial response. *Science* **2006**, *311*, 1770–1773.

(26) Peng, J. B.; Chen, X. Z.; Berger, U. V.; Weremowicz, S.; Morton, C. C.; Vassilev, P. M.; Brown, E. M.; Hediger, M. A. Human calcium transport protein CaT1. *Biochem. Biophys. Res. Commun.* **2000**, *278*, 326–32. Wood, R. J.; Tchack, L.; Taparia, S. 1,25-Dihydroxyvitamin D₃ increases the expression of the CaT1 epithelial calcium channel in the Caco-2 human intestinal cell line. *BMC Physiol.* **2001**, *1*, 11.

(27) Wu, Q.; Burghardt, R.; Safe, S. Vitamin D-interacting protein 205 (DRIP205) coactivation of estrogen receptor alpha (ERalpha) involves multiple domains of both proteins. *J. Biol. Chem.* **2004**, *279*, 53602–53612.

(28) (a) Shimizu, M.; Miyamoto, Y.; Takaku, H.; Matsuo, M.; Nakabayashi, M.; Masuno, H.; Udagawa, N.; DeLuca, H. F.; Ikura, T.; Ito, N. 2-Substituted-16-ene-22-thia-1alpha,25-dihydroxy-26,27-dimethyl-19-norvitamin D₃ analogs: Synthesis, biological evaluation,

and crystal structure. *Bioorg. Med. Chem.* **2008**, *16*, 6949–6964. (b) Vanhooke, J. L.; Benning, M. M.; Bauer, C. B.; Pike, J. W.; DeLuca, H. F. Molecular structure of the rat vitamin D receptor ligand binding domain complexed with 2-carbon-substituted vitamin D₃ hormone analogues and a LXXLL-containing coactivator peptide. *Biochemistry* **2004**, *43*, 4101–4110. (c) Rochel, N.; Wurtz, J. M.; Mitschler, A.; Klaholz, B.; Moras, D. The crystal structure of the nuclear receptor for vitamin D bound to its natural ligand. *Mol. Cell* **2000**, *5*, 173–179. (d) Ciesielski, F.; Rochel, N.; Moras, D. Adaptability of the Vitamin D nuclear receptor to the synthetic ligand Gemini: remodelling the LBP with one side chain rotation. *J. Steroid Biochem. Mol. Biol.* **2007**, *103*, 235–242. (e) Tocchini-Valentini, G.; Rochel, N.; Wurtz, J. M.; Mitschler, A.; Moras, D. Crystal structures of the vitamin D receptor complexed to superagonist 20-*epi* ligands. *Proc. Natl. Acad. Sci. U. S. A.* **2001**, *98*, 5491–5496. (f) Eelen, G.; Valle, N.; Sato, Y.; Rochel, N.; Verlinden, L.; De Clercq, P.; Moras, D.; Bouillon, R.; Muñoz, A.; Verstuyf, A. Superagonistic fluorinated vitamin D₃ analogs stabilize helix 12 of the vitamin D receptor. *Chem. Biol.* **2008**, *15*, 1029–1034.

(29) Smith, C. L.; O'Malley, B. W. Coregulator function: a key to understanding tissue specificity of selective receptor modulators. *Endocr. Rev.* **2004**, *25*, 45–71.

(30) Kaneko, E.; Matsuda, M.; Yamada, Y.; Tachibana, Y.; Shimomura, I.; Makishima, M. Induction of Intestinal ATP-binding Cassette Transporters by a Phytosterol-Derived Liver X Receptor Agonist. *J. Biol. Chem.* **2003**, *278*, 36091–36098.

(31) Tavangar, K.; Hoffman, A. R.; Kraemer, F. B. A micromethod for the isolation of total RNA from adipose tissue. *Anal. Biochem.* **1990**, *186*, 60–63.

(32) Otwinowski, Z.; Minor, W. Processing of X-ray diffraction data collected in oscillation mode. *Methods Enzymol.* **1997**, *276*, 307–326.

(33) Brunger, A. T.; Adams, P. D.; Clore, G. M.; DeLano, W. L.; Gros, P.; Grosse-Kunstleve, R. W.; Jiang, J. S.; Kuszewski, J.; Nilges, M.; Pannu, N. S.; Read, R. J.; Rice, L. M.; Simonson, T.; Warren, G. L. Crystallography & NMR system: a new software suite for macromolecular structure determination. *Acta Crystallogr., Sect. D: Biol. Crystallogr.* **1998**, *54* (Pt 5), 905–921.

(34) McRee, D. E. XtalView Xfit—a versatile program for manipulating atomic coordinates and electron density. *J. Struct. Biol.* **1999**, *125* (2–3), 156–165.